

**J. L. Bouvard**

e-mail: jeanluc@cavs.msstate.edu

**D. K. Ward**

**D. Hossain**

Center for Advanced Vehicular Systems,  
Mississippi State University,  
200 Research Boulevard,  
Starkville, MS 39759

**S. Nouranian**

Dave C. Swalm School of Chemical Engineering,  
Mississippi State University,  
Mississippi, 39762

**E. B. Marin**

**M. F. Horstemeyer**

Center for Advanced Vehicular Systems,  
Mississippi State University,  
200 Research Boulevard,  
Starkville, MS 39759

# Review of Hierarchical Multiscale Modeling to Describe the Mechanical Behavior of Amorphous Polymers

*Modern computational methods have proved invaluable for the design and analysis of structural components using lightweight materials. The challenge of optimizing lightweight materials in the design of industrial components relates to incorporating structure-property relationships within the computational strategy to incur robust designs. One effective methodology of incorporating structure-property relationships within a simulation-based design framework is to employ a hierarchical multiscale modeling strategy. This paper reviews techniques of multiscale modeling to predict the mechanical behavior of amorphous polymers. Hierarchical multiscale methods bridge nanoscale mechanisms to the macroscale/continuum by introducing a set of structure-property relationships. This review discusses the current state of the art and challenges for three distinct scales: quantum, atomistic/coarse graining, and continuum mechanics. For each scale, we review the modeling techniques and tools, as well as discuss important recent contributions. To help focus the review, we have mainly considered research devoted to amorphous polymers. [DOI: 10.1115/1.3183779]*

## 1 Introduction

As energy consumption becomes a larger concern for industry and consumers, a significant amount of research is devoted to saving fuel and reducing the cost of production. Developing new lightweight materials, such as magnesium alloys and polymers, is one method of cutting fuel use, particularly in industries associated with transportation. One class of such lightweight materials is amorphous polymers. They are important engineering materials widely used in industry because of their physical, optical (light transparency), and mechanical properties (toughness). Furthermore they are relatively inexpensive. Along with cutting energy costs, designers also seek to reduce the amount of expensive mechanical testing, e.g., crash tests, as well as time consuming material testing encompassing a wide variety of environmental and loading conditions. Computational methods offer an excellent opportunity to cut cost and predict material response over a much larger range of conditions that could ever be examined through experiments. In order to predict material properties over large ranges of temperatures, strain rates, and stress states, material microstructure and underlying molecular mechanisms must be understood. Multiscale modeling is one such computational technique that incorporates properties associated with the smallest length and time scales into the design of components [1]. For the case of metals, multiscale modeling has been rigorously developed and has proven fruitful in the development of automotive components [2,3]. There are two types of multiscale models: concurrent and hierarchical. The former contains multiple models in a single simulation that run seamlessly and pass information between each other through a “hand shaking” procedure [4–6],

while hierarchical modeling uses separate simulations to compute structure-property relations at one length scale in order to pass the “effect” to higher length scales [1–3,7].

As depicted in Fig. 1, different length and time scales are associated with a multiscale modeling methodology. At the smallest scale is quantum mechanics, with relevant lengths of angstroms and time scales of  $10^{-15}$  s, while at the largest scale (continuum mechanics) lengths can exceed meters and the times can approach years (in some cases,  $10^9$  s). For the case of metals, the length scales have been nearly linked—through different mechanisms, dislocations for plasticity, and voids/particles for fracture [8]. The hierarchical multiscale modeling scheme for metals includes energy potentials determined from quantum mechanics (QM) that atomistic simulations use to examine dislocation nucleation, mobility, and interactions. Discrete dislocation dynamics then use the dislocation mobilities found from atomistic simulations to study dislocation networks and structure development for work hardening. As such, the outputs from dislocation dynamics then assist in developing polycrystalline plasticity work hardening models and ultimately macroscale continuum level internal state variable (ISV) models for use in component level simulations.

For amorphous polymers, hierarchical modeling is in a fairly primitive state relative to their metallic counterparts. Length and time scales encountered in polymers range over several orders of magnitude. The lengths scales associated with a single polymer chain include a single chemical bond ( $<10$  nm), the persistence length, or the Kuhn length [9] of the polymer that consists of a segment of the polymer chain with several chemical bonds ( $\approx 100$  nm), and the radius of gyration ( $R_g$ ) ( $\approx 1000$  nm) [10]. Additional length scales are encountered in polymer melts comprising millions of polymeric chain molecules. The associated time scales for the relaxation phenomena of the entangled polymer chains also add complexity to multiscale modeling. The relaxation of polymer chains is temperature and pressure dependent and involves different modes of motions. At the smaller length scales, vibrations of a single C–C bond (for example, in polyethylene (PE)) or the bond

Contributed by the Materials Division of ASME for publication in the JOURNAL OF ENGINEERING MATERIALS AND TECHNOLOGY. Manuscript received February 16, 2009; final manuscript received June 18, 2009; published online September 1, 2009. Review conducted by Hussein Zbib.

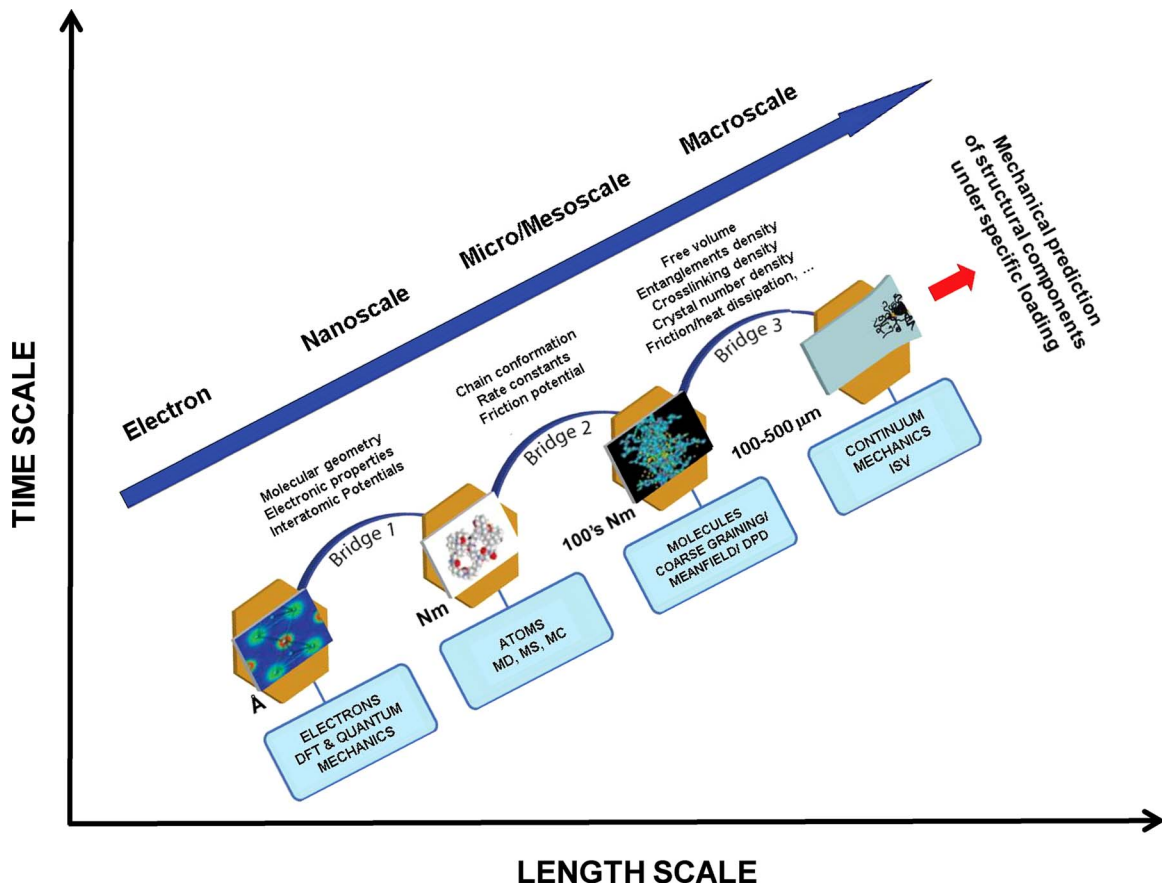


Fig. 1 Schematic of a general hierarchical modeling approach for polymers

angle  $\theta$  ( $\approx 10^{-13}$  s) occur alongside torsional *gauche-trans* transformations, which happen at a much slower rate ( $\approx 10^{-11}$  s) [10]. The aforementioned motions contributing to the conformational or entropy changes lead to short length relaxations but do not equilibrate the persistence length and radius of gyration of the polymer. Since polymers do not have a single deformation mechanism, such as dislocations, to be followed through all length scales and deformation mechanisms span larger length and time scales, the problem of multiscale modeling is a larger more complex task. The huge span of length and time scales exhibited by polymers is a perfect example for the importance of multiscale modeling in these materials.

This review will focus on the current state of hierarchical multiscale modeling to describe the mechanical behavior of amorphous polymers, primarily an amorphous PE and polycarbonate (PC). A variety of polyethylenes exist depending on the extent of chain branching, which in turn influences the degree of crystallinity. However, this review is focused on an idealized linear amorphous PE. Section 2 covers computational chemistry using quantum mechanics to determine structures and properties for atomistic simulations. Next, in Sec. 3, we review associated molecular dynamic simulations. This section also includes a brief discussion of several coarse-graining methods with a particular focus on bead-spring methods. Section 4 covers continuum methods, specifically internal state variable models. Each section contains information on theory, modeling techniques, current state of the art, and a discussion of the information that is passed to the next length scale.

## 2 Quantum Mechanics

The foundation of multiscale modeling is based on QM. QM calculations provide the essential parameters such as bond

lengths, bond angles, dihedral angles, and force field potentials essential for describing the interactions between the building blocks in polymer materials. Developing interatomic potentials based on conformations and energies calculated using QM creates a method for performing molecular simulations, which provide accurate polymers material properties. This section focuses on the smallest length and time scales associated with QM. We begin by discussing the fundamental background of quantum mechanics followed by a brief introduction of ab initio and semi-empirical quantum mechanics, followed by a section describing in detail the density functional theory (DFT) as one method for solving QM problems. We finally discuss some current work conducted using QM to model and understand polymers (Sec. 2.2) through information passing techniques.

**2.1 Quantum Mechanics Background.** The basis for material properties is related to the interactions of the electrons and nuclei that comprise a structure. These interactions generally follow the fundamental laws of QM. Quantum mechanical methods, which are applicable for studying a wide range of physical properties in different systems, are based on solving for the wave function from the Schrödinger equation (SE) [11]:

$$H\psi = E\psi \quad (1)$$

where  $\psi$  is the wave function of the system,  $H$  is a Hamiltonian, and  $E$  is an eigenvalue of the wave function.

For multi-electron systems, the Hamiltonian is very complicated and solving for an exact solution is not practical. Thus, to solve SE for the wave function and to study the physical properties of materials, nonempirical ab initio methods take advantage of the Born-Oppenheimer approximation (BOA) [11–14]. The BOA solves SE by considering the nuclear motion and electron motion independently [11]. Ab initio simulations can accurately deter-

mine system energies, but these simulations are very computationally expensive; thus, the models are restricted to a small number of atoms, simulated for only a few picoseconds. Empirical or semi-empirical quantum-mechanical methods have also been developed to predict material properties theoretically. Among the QM methods, the most commonly used ones for engineering materials are based on DFT.

**2.1.1 Ab Initio Quantum Mechanical Methods.** Ab initio quantum-mechanical methods are based on solving for the wave function of electrons in the SE. In these methods, no empirical data are used. The simplest ab initio electronic structure calculation method is the Hartree-Fock (HF) method [11–13]. However, the shortcoming of HF electron correlation is not considered. To address this limitation, several methods called “post-HF” methods [11–18] were developed. Some of these important methods are the Møller-Plesset perturbation (MPn) theory [11–14], configuration interaction (CI) [11–13,15], coupled cluster (CC) theory [11–13,16], multiconfiguration self-consistent field (MCSCF) [11–13,17,18], and complete active space self-consistent field (CASCF) [11–13].

**2.1.2 Semi-Empirical Quantum Mechanical Methods.** Semi-empirical quantum-mechanical methods are based on HF. However, some approximations are made and many parameters are used from empirical data. Another common feature of semi-empirical methods is that only the valence electrons are considered. The important semi-empirical methods are complete neglect of differential overlap (CNDO) [19–22], intermediate neglect of differential overlap (INDO) [23], modified neglect of diatomic overlap (MNDO) [24], modified intermediate neglect of differential overlap (MINDO) [25], and Austin Model 1 (AM1) [26]. Semi-empirical methods are fast compared with HF and post-HF methods. These methods are used to produce qualitative and quantitative results on larger molecules than are possible for ab initio quantum methods. These methods are useful for predicting the structure and electronic properties of large organic molecules.

**2.1.3 DFT.** DFT [27–33] has proved to be a very powerful quantum-mechanical method for investigating the electronic structure of atoms, molecules and solids, and is much simpler and less expensive, computationally, relative to other ab initio and semi-empirical quantum-mechanical methods [11,12]. DFT is essentially based on two theorems of Hohenberg and Kohn [29,30]: The ground-state wave function,  $\psi$ , is a unique functional of the electron density  $\rho(\mathbf{r})$  and a defined energy functional is minimized by the ground-state electron density  $\rho_0$ . Applying the Hohenberg and Kohn theorems results in a total energy expressed by

$$E = T[\rho] + \int V_{\text{ext}}\rho(\mathbf{r})d\mathbf{r} + \frac{1}{2} \iint \frac{\rho(\mathbf{r})\rho(\mathbf{r}')}{|\mathbf{r} - \mathbf{r}'|} d\mathbf{r}d\mathbf{r}' + E_{\text{xc}}[\rho] \quad (2)$$

where  $T[\rho]$  is the kinetic energy of a system of noninteracting electrons with density  $\rho(\mathbf{r})$ ,  $V_{\text{ext}}$  is the external potential of electron and neutron interactions, the third term corresponds to electron-electron interaction potentials, and  $E_{\text{xc}}[\rho]$  is the electron exchange-correlation energy of an interacting system with density  $\rho(\mathbf{r})$  at position  $\mathbf{r}$ . Kohn and Sham [30] then showed that summing the squares of the wave function solutions of  $N$  noninteracting Schrödinger equations give the charge density

$$\rho(\mathbf{r}) = \sum_{i=1}^N |\varphi_i(\mathbf{r})|^2 \quad (3)$$

where  $\varphi_i(\mathbf{r})$  is the wave function for Schrödinger equation associated with electron  $i$  or

$$\left(-\frac{1}{2}\nabla^2 + v_{\text{eff}}(\mathbf{r})\right)\varphi_i(\mathbf{r}) = \varepsilon_i\varphi_i(\mathbf{r}) \quad (4)$$

where  $v_{\text{eff}}$  is the effective external potential and  $\varepsilon_i$  are the eigenvalues, which have no physical meaning on their own but the sum is related to the total energy through

$$E = \sum_i^N \varepsilon_i - V_H[\rho] + E_{\text{xc}}[\rho] - \int \frac{\delta E_{\text{xc}}[\rho]}{\delta \rho(\mathbf{r})} \rho(\mathbf{r})d\mathbf{r} \quad (5)$$

One source of inaccuracy from these methods is the definition of the exchange-correlation energy. For an arbitrary  $\rho(\mathbf{r})$ , the exact expression for  $E_{\text{xc}}[\rho]$  is unknown. However, if  $\rho(\mathbf{r})$  varies sufficiently, one can write

$$E_{\text{xc}}[\rho] = \int \rho(\mathbf{r})\varepsilon_{\text{xc}}(\rho(\mathbf{r}))d\mathbf{r} \quad (6)$$

where  $\varepsilon_{\text{xc}}(\rho)$  is the exchange and correlation energy per electron of a uniform electron gas of density  $\rho$ .

Several approximations for the exchange-correlation energy have been developed to make DFT applicable for materials science. The most successful exchange-correlation approximations are local density approximation (LDA) [30,31] or local-spin-density approximation (LSDA) [34], and generalized gradient approximation (GGA) [31,34]. LSDA determines the exchange-correlation energy by assuming that the exchange-correlation energy  $\varepsilon_{\text{xc}}$  for an electron at a point  $\mathbf{r}$  in the electron gas is equal to the exchange-correlation energy per electron in an electron gas of uniform spin densities of  $\rho_{\uparrow}, \rho_{\downarrow}$  (the arrow indicates the spin direction):

$$E_{\text{xc}}^{\text{LSDA}}[\rho_{\uparrow}, \rho_{\downarrow}] = \int \rho(\mathbf{r})\varepsilon_{\text{xc}}^{\text{unif}}(\rho_{\uparrow}, \rho_{\downarrow})d\mathbf{r} \quad (7)$$

where  $\varepsilon_{\text{xc}}^{\text{unif}}(\rho_{\uparrow}, \rho_{\downarrow})$  is the exchange-correlation energy per unit volume of a homogeneous electron gas of density  $\rho(\mathbf{r})$ .

LSDA, in principle, ignores corrections to the exchange-correlation energy at a point  $r$  due to nearby inhomogeneities in the electron gas [35]. To improve the error of LDA or LSDA, a more accurate GGA [17,19,20] was developed. The exchange-correlation energy term for GGA is

$$E_{\text{xc}}^{\text{GGA}}[\rho_{\uparrow}, \rho_{\downarrow}] = \int \varepsilon(\rho_{\uparrow}, \rho_{\downarrow}, \nabla\rho_{\uparrow}, \nabla\rho_{\downarrow})d\mathbf{r} \quad (8)$$

where  $\nabla\rho$  is the gradient of the electron density. The GGA is more accurate than LDA for predicting the properties of materials.

Other DFT methods used for predicting materials properties are m-GGA [36], hyper-GGA [37], and hybrid density functional [38]. Approximations involving gradient corrections that have been studied extensively include the exchange functionals B (Becke) [39], FT97 (Filatov-Thiel) [40], mPW (Adamo-Barone) [38], and the correlation functionals of P (Perdew) [32] and of LYP (Lee-Yang-Parr) [41], PBE (Perdew-Burke-Ernzerhof) [42], and PW91 (Perdew-Wang) [43]. Combinations of these forms for the exchange and correlation energy are often referred to as “BP” and “BLYP,” “BPW91” approximations. In a hybrid functional, a mixture of HF exchange and GGA exchange is used in combination with GGA and/or LDA correlation. For instance, the most widely used hybrid functional is B3LYP (Becke three-parameter hybrid functional combined with LYP functional) [44].

DFT is one theory in which the material’s energy is expressed as a function of the electron density or spin density. The DFT within LSDA and GGA, in general, works well for ground-state properties of moderately correlated systems such as total energies, energy difference, cohesive energies, atomization energies, surface energies, energy barrier, atomic structure, and magnetic moments of real materials [32–34]. Density functional calculations also provide a method of calculating structural, electronic, and binding properties of molecules. Yet, DFT methods have limita-



tions when predicting the excited state and spectroscopic properties of the systems. For example, band gaps of semiconductors are extremely underestimated because they are related to the properties of excited states [45,46].

**2.2 Current State of Quantum Mechanics in Multiscale Modeling of Polymers.** Here we discuss a few examples of applying quantum mechanics for predicting properties and passing them to higher length scales. One of the most important polycarbonates is bisphenol A polycarbonate (BPAPC). With outstanding optical and mechanical properties, BPAPC is an important material for manufacturing and design. With respect to multiscale modeling, one major interest of studying BPAPC is the influence of chain segment motion on intermolecular interactions. The  $\pi$ -flip of the phenylene rings in immobile [47] and mobile [48] forms is the central issue in BPAPC and its analogs. Only a few quantum-mechanical calculations done on polycarbonates and their analogs have been performed with the aim to generate force fields of BPAPC [49–59].

Many studies using quantum mechanics have focused on the structure and energies of polycarbonate dating back to the early 1960s [49]. The primary focus of these studies was to calculate ground-state conformational energies and ring flips of the phenyl ring [50–59]. Overall, the DFT calculations of ground-state geometries, vibrational frequencies, and energy barriers showed good agreement with available experimental results. With respect to multiscale modeling, QM creates the foundation for the higher length scales. Developing interatomic potentials based on QM establishes the link to the next length scale. Not all developed interatomic potentials incorporate information from QM but a few have successfully created potentials based on QM [60–65]. Early attempts at creating accurate potentials from QM fit predetermined functions (similar to the form discussed later in Sec. 3.2.2) to a theoretical Hessian and experimental data [62]. This early work also used empirical formulations to develop nonbonded van der Waals interactions. Using a combination of QM and empirical methods has benefits since the weak nonbonded interactions are very difficult to calculate using QM techniques [63]. Later simulations included other optimization criterion including elastic constants and internal stresses [65] in addition to the QM quantities. The previously mentioned potentials were generally used for simple linear polyethylene like polymers but are not limited to them. For more complicated polymers, such as PC, the potentials should take into account the energy barriers for more complicated conformation changes, like the phenyl ring flip [61]. This gives just a sample of the different potentials developed over the years. A detailed description of the form for one potential is given in Sec. 3.2.2. Refining and increasing the accuracy of the predictions for the material response are a continuing effort. These QM informed potentials are now a useful input for running larger molecular simulations such as atomistic and coarse-grain methods at the micro- and macroscales.

### 3 Atomistic-Mesoscale Modeling: Molecular Dynamics and Coarse Graining

This section will describe the techniques and current state of modeling polymers as a series of interacting particles using MD. Here, the discussion will begin with an overview of MD theory. MD includes both general atomistic models where every atom is represented by a particle as well as coarse-grained models, which use a single particle to describe the motion of several atoms. The theory is followed by methods for creating initial structures of amorphous polymers and descriptions of the atomic potentials used to describe the interactions between particles. Following the theory, we present a sample of other coarse-graining techniques. A few statements then address the issue of bridging time scales. Section 3.1 describes the current state of the atomistic modeling while Sec. 3.4 reviews some of the current “bottom-up” hierarchical methods that use MD.

**3.1 Molecular Dynamic Modeling Theories.** Molecular dynamics modeling follows the motion of a collection of particles through time and space by numerically integrating Newton's equations of motions. In order to progress the simulation in time, the energy for the entire system is expressed as a series of interactions between particles (the interaction potentials are described in detail in Sec. 3.2). The forces on each particle are then determined by taking the derivative of the system energy,  $E$ , with respect to the position vector for a particle pair,  $\mathbf{r}_i$ , as  $\mathbf{f}_i = \partial E / \partial \mathbf{r}_i$ . Once the forces on each particle due to the interaction of the other particles in the system are determined, the equations are integrated using any number of schemes, most notably the Verlet [66] and Gear velocity operator methods [67]. These schemes are shown to be stable and conserve energy very well relative to other methods [67]. MD in the simplest form addresses problems consisting of a constant number of atoms, volume, and energy,  $NVE$ . Examining a system of constant energy and volume limits the possible data that is collected from the model. To expand the sample space for MD simulations, a series of methods has been developed that allow for temperature and pressure control of the system, such as  $nvt$  [68,69], constant number of atoms, volume, and temperature, and  $NPT$ , constant number of atoms, pressure, and temperature, dynamics. For further explanation of the molecular dynamics models and methods of running these simulations, see Ref. [67]. Not all dynamic models are limited to interactions between single atoms but can be extended to larger molecules, comprising several atoms, interacting with other large molecules. These larger length scale models, or coarse-grained models, include a united atom motion, which generally combines two to four atoms into a single particle [70–75], and bead-spring methods, which combine many more groups of atoms into particles and springs [76–80]. One example of the software that includes many potentials and a majority of the machinery necessary to perform MD simulations is large-scale atomic/molecular massively parallel simulator (LAMMPS) [81]. LAMMPS is free to download and is capable of modeling full atomistic simulations and some bead-spring type models.

### 3.2 Modeling Details

**3.2.1 Initial Structures.** An important component of atomic simulations of polymers is the initial position of the particles. In order to have a “statistically” representative initial structure, the conformations should have a Boltzmann distribution at the defined temperature. For the simple case of polyethylene, one method to create an initial structure is a Monte Carlo (MC) random walk, which randomly selects an initial start position and then grows each chain according to a probability for each possible direction of growth. The probability is determined by the local density of neighbor particles, as well as the resulting conformation [82–84]. These methods become more complicated when introducing cross-links into the system, but similar growths can be performed to generate cross-linked materials. More complicated polymers such as polycarbonate use the same methodology requiring a Boltzmann distribution of the conformations from a Monte Carlo random walk [77,78].

**3.2.2 Interatomic Potentials.** As described in Sec. 2, MD simulations require an accurate interatomic potential. Mayo et al. [85] developed a generic potential, the Dreiding potential, to describe interactions between most nonmetallic elements. Unlike other atomic potentials, the Dreiding potential does not depend on the particular type of atoms in the bonding but rather on the type of bonds present. The potential is described by individual force constants and geometric parameters that depend on the bond hybridization and effectively models all combinations of atoms. This potential has two components: the valence or bonded interactions ( $E_{val}$ ), for atoms chemically bonded to one another, and the non-bonded interactions ( $E_{nb}$ ), for the interactions not chemically bonded to one another. The total energy is expressed as the sum of these two terms:

$$E = E_{\text{val}} + E_{\text{nb}} \quad (9)$$

The valence term of the energy is further broken up into the sum of four types of bonded interactions: bond stretch ( $E_B$ ), bond angle bend ( $E_A$ ), dihedral angle torsion ( $E_T$ ), and inversion terms ( $E_I$ ). The nonbonded interactions also consist of the sum of several components such as, but not limited to, van der Waals ( $E_{\text{vdW}}$ ), electrostatic ( $E_Q$ ), and hydrogen bonds ( $E_{\text{hb}}$ ).

Each bonded component of the energy has a multitude of forms to express the energy, but here the focus will be those presented by Mayo et al. [85]. The bond stretch is a two body interaction, where only two particles are involved in the energy calculation, using a harmonic formulation:

$$E_B = \frac{1}{2}k_e(R - R_e)^2 \quad (10)$$

where  $k_e$  is the force constant,  $R$  is the bond length, and  $R_e$  is the equilibrium bond length. Another potential mentioned for the bond stretch is the Morse [86,87] potential, which is more accurate and allows for bond breaking at an energy of  $D_e$ .

$$E_B = D_e[e^{-(\alpha R - R_e)} - 1]^2 \quad (11)$$

In this case the force constant is expressed as  $\alpha = [k_e/2D_e]^{1/2}$ . For the angle  $\theta_{ijk}$  between bonds,  $IJ$  and  $JK$ , a simple harmonic is again used to express the energy as the following:

$$E_A = \frac{1}{2}C_{IJK}[\cos \theta_{IJK} - \cos \theta_j^0]^2 \quad (12)$$

This is a three-body interaction involving the three nearest neighbors in the calculation, where  $C_{IJK}$  is the force constant, and  $\theta_j^0$  is the equilibrium angle from either known equilibrium structures or quantum mechanics simulations.

The torsion interaction, a four-body term, is expressed as

$$E_T = \frac{1}{2}V_{JK}\{1 - \cos[n_{JK}(\varphi - \varphi_{JK}^0)]\}^2 \quad (13)$$

The dihedral angle,  $\varphi$ , is the angle between the  $IJK$  and  $JKL$  planes,  $n_{JK}$  is the periodicity,  $V_{JK}$  is the energy barrier to rotation, and  $\varphi_{JK}^0$  is the equilibrium rotation. In the case of polyethylene, three possible minima exist: one *trans* and two *gauche* conformations. The Dreiding potential captures the conformation distribution very well.

Since the inversion term is not always applicable, the inversion energy can also be represented by a harmonic similar to Eqs. (10) and (11). While the nonbonded interactions can contain many components including electrostatics and hydrogen bonding, we will only address the van der Waals component. The van der Waals interaction, just as the other components, can have a range of forms but is usually expressed as either a 12–6 or a 9–6 Lennard-Jones [67,88] potential. A Lennard-Jones 12–6 type is given by the following:

$$E_{ij,\text{vdW}} = 4\varepsilon \left[ \left( \frac{\sigma}{r_{ij}} \right)^{12} - \left( \frac{\sigma}{r_{ij}} \right)^6 \right] \quad (14)$$

where  $\varepsilon$  is the energy well of the potential,  $\sigma$  is the zero energy spacing for the potential, and  $r_{ij}$  is the distance between particles  $i$  and  $j$ .

Mayo et al. [85] included an extensive list of values for all of the constants included in each potential, for many different types of hybridization and initial structures. With the Dreiding potential and many others, a wide range of molecules can be modeled for systems containing  $>10^6$  atoms or “united atoms” on parallel computers. The most generic united atom model lumps the H atoms associated with each C backbone atom of polyethylene creating a single united atom for each methyl group. As an example, of computational costs, running LAMMPS [81] on 128 processors at Mississippi State University’s Center for Advanced Vehicular Systems  $10^6$  atoms simulated for 1 ns takes 72 h.

The Dreiding potential is not limited to single atom-atom interactions but can be extended to molecule-molecule interactions, also known as the united atom methods. The most generic united

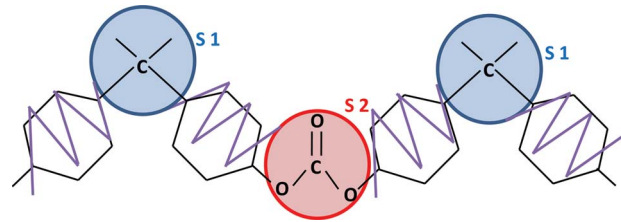


Fig. 2 Mapping of a polycarbonate chain onto a two bead-spring coarse-grain model

atom model lumps the H atoms associated with each C backbone atom of polyethylene creating a single united atom for each methyl group.

With the potentials developed using QM methods including the aforementioned Deidre as well as CHARMM [89,90], AMBER [91], and many others not mentioned here, a number of different polymers are now modeled at the atomistic level. These potentials capture structure and energetic barriers very well but some limitations do exist in the prediction of the van der Waals and nonbonded interactions. Also, terminal methyl groups are modeled the same as the interior groups, which can lead to incorrect free volume predictions. Yet, atomistic MD simulations allow for simple calculations to be performed on polymer melts and in some cases mechanical properties of glassy amorphous linear polymers. Care needs to be taken when these results are passed onto larger length scales because the length and times scales limit the mechanisms that are responsible for the majority of the viscoelastic/plastic properties of the material, primarily reptation [92]. Reptation or snakelike motion is one of the fundamental concepts of polymer dynamics in entangled polymer systems, which is used to describe many physical phenomena associated with viscoelastic responses of these systems. For a detailed discussion on how to incorporate the reptation theory and entropic effects associated with it in a MD simulation of entangled polymer systems, the reader can refer to Ref. [10].

**3.2.3 Coarse-Graining: Bead-Spring.** In most cases the bond stretch and bond angle potentials are very stiff relative to the torsional and van der Waals potentials. Thus, often the bond stretch and bond angle are considered rigid and allowing for further coarse-graining as previously mentioned for polycarbonate. Coarse-graining is a method of modeling that further increases the length scales studied using MD but is still constrained by time scaling. The coarse-graining methods discussed here will focus on bead-spring methods; yet many other methods do exist including Monte Carlo methods [93], Brownian dynamics models [94], and dissipative particle dynamics [95].

As previously stated, for simplicity, the bead-spring discussion will focus on models for polycarbonate. The first bead-spring methods were simple extensions of the united atom method [76] and used Monte Carlo methods, as well as rotational isomeric state models [96], to create representative initial structures. Tschöp et al. [77] developed a coarse-graining method for polycarbonate that implemented conformation distribution functions dependent on different geometric characteristics of the polymer chains. For this model, a polycarbonate chain was represented by two types of particles, as shown in Fig. 2. The center of mass for the two particles, S1 and S2, are centered on the geometric center of isopropylidene group and the carbonate group, respectively. Each distribution function is then directly proportional to the Boltzmann factors of the generalized intrachain interaction potentials. These potentials then generate tables for use in the united atom method. Using these particular coarse-grained methods requires no fitting parameters and the conformational properties of the polymer remain. Yet, some issues can arise using coarse-graining, namely, generating the tables for each type of polymer over a

range of temperatures. Tschöp et al. [78] also presented a method to reverse the coarse-graining that is useful to recapture the atomistic details of the polymer.

Meyer et al. [97] took the coarse-graining procedure a step further by focusing on the interparticle potentials and creating a function that correctly reproduces the radial distribution function (RDF) for the trajectory of the nonbonded particles during a polymer melt. The functions presented by Meyer et al. [97] are based on a standard Lennard-Jones potential but include four to five degrees of freedom for more interactions. Meyer et al. [97] also presented a method for automating the process of generating the distribution functions for the geometric distribution of the polymer chains. The automated process must be approached with care since predictions can give solutions to local structural minima rather than the true global minimum.

Abrams and Kremer [98] later showed that issues arose with coarse-graining polycarbonate using just two types of beads. Artifacts in the melt structure near interfaces appeared, but with introducing two additional beads this problem was resolved. Many of the numerical artifacts arise from the relation of the bead volume relative to the bond length [98,99]. This appears as a step back for the coarse-graining simulation process, but considerable increases in the size of simulation still exist relative to full molecular dynamics.

While bead-spring modeling does simulate larger structures and longer lengths of time, they are still extremely limited when it comes to polymeric materials. Another class of coarse-grain models includes MC simulations. Unlike MC simulations for metals, polymers are not strictly limited to a predetermined lattice but rather to local chain conformations that are probable [94]. MC methods advance the simulation according to a series of steps associated with a jump rate that alters the conformation of the chain by altering dihedral angles and chain-to-chain connectivity. These methods greatly decrease the amount of time it takes to relax a structure and also allow for reptation processes to occur.

**3.2.4 Other Mesoscale Models.** The microscale to mesoscale bridge often times is vaguely defined. The mesoscale is primarily defined by the entropic considerations of the chain packing and conformation [100]. Kremer's definition of mesoscale models is essentially coarse-graining including the methods discussed above. A few examples of other mesoscale models include Brownian dynamics (BD) [79,101], dissipative particle dynamics (DPD) [96,102–104], and dynamic density functional theory (DDFT) [105] models for molecules in solvent. BD and DPD methods essentially work the same way as a bead-spring model but capture diffusive effects typical for molecules suspended in solution. Furthermore, DPD captures hydrodynamic effects because it conserves momentum. Removing the particles associated with the suspending fluid and introducing a dissipative force greatly reduce the computational requirements. DDFT models tend to focus more on phase separation and copolymer evolution than on the mechanical response of a homopolymer. These models help bridge the gap for many types of heterogeneous materials but do not significantly advance the study of the polymers of interest here.

**3.2.5 Time Scale Issues and Accelerated Dynamics.** Differences in time scales for different mechanisms should always be a consideration when developing multiscale models. As previously mentioned, various mechanisms act up to ten orders of magnitude just to reach a relaxed state. For a melt of short nonentangled polymer chains, the relaxation time of a polymer chain with an  $N_p$  degree of relaxation,  $\tau_{N_p}$ , can be approximated by the Rouse model,

$$\tau_{N_p} = \tau_1 N_p^2 \quad (15)$$

where  $\tau_1$  is the relaxation time for a polymer with a single repeat unit [10]. This means that as chains increase in size, the computational time necessary to relax the system becomes unreasonable. The situation becomes worse by introducing entanglements into

the structure. For this case, reptation theory predicts a relaxation time proportional to  $N_p^3$  as given by the following:

$$\tau_{N_p} = \tau_1 \left( \frac{N_p}{N_p^e} \right) N_p^2 \quad (16)$$

where  $N_p^e$  is the number of repeating units required for the entanglement [10]. For a moderate degree of polymerization, say,  $N_p=500$ , the relaxation time increases by almost eight orders of magnitude ( $\approx 10^{-5}$  s). Therefore, MD simulations of polymer systems would need enormous computer power and time if all relevant relaxations are to be considered in full detail. The limitations of current computational capabilities limit the amount of time (a few nanoseconds) an MD simulation can run. Other options exist that have similar detail as MD, but they either increase the amount of time simulated by the model or increase the frequency of mechanisms that become active. Transition state theory (TST) offers one method for resolving the time scale issue inherent in MD [106]. TST computes motion in much the same way a MC simulation does by jumping a system from one state to another. The frequency of state changes the overall time scale of the system at a rate much higher than the vibrations with in an energy minimum. Unfortunately, TST requires some knowledge of the states and the energy profile a priori. For most polymer simulations, only a selected few state changes are known beforehand, such as dihedral rotations or phenyl ring flips. Using only these selected few state changes does not ensure that the material progresses in time realistically. The shortcomings of TST led to the development of other methods that do not require previous knowledge of the deformation mechanisms. Hyperdynamics (HD) or accelerated dynamics uses modifications to the energy profile to move the dynamics along more quickly [107,108]. HD introduces an energy bump to the well of an initial state. This method does not limit the type of state change that can occur. The overall system evolves in a realistic fashion only at an accelerated rate. These simulations do lose the actual time progressed but time can be statistically represented by the number of events that have occurred. Two other models that do not work as well but require mentioning are on-the-fly kinetic Monte Carlo (kMC) [109] and temperature accelerated dynamics (TAD) [110]. kMC also resolves the requirement of knowing the deformation mechanisms a priori. This model searches the entire energy space for any saddle points that could lead to a state change and catalogs the energy differences to be used in a kMC simulation. This simulation requires a significant amount of computation power for large systems containing several state changes per step. The TAD adds a boost to the energy just as HD does but through raising the temperature of the system. Raising the temperature introduces unbalanced energy changes for the different mechanisms in the system. These unbalanced energy changes eventually lead to incorrect rate of state changes between mechanisms. The HD method and TST method have also been combined to boost only the energy wells for known mechanisms [84]. Several other methods exist following similar lines to those discussed here [111–114].

**3.3 Current State of Molecular Dynamic Simulations of Polymers.** Much work has been done at the atomistic level to ensure that the current methods do indeed effectively capture the correct polymer response under glassy high strain rate conditions. Most of this modeling has focused on united atom methods for polyethylenes, since they have the simplest chemical structure of all polymers. With a carbon backbone that has two hydrogen atoms bonded to each carbon atom, initial structures are generated with little difficulty. Polycarbonate is another popular material because of its many practical uses but requires a somewhat more sophisticated bead-spring model. It is impossible to report on all of the studies that use MD to examine the atomistic deformation mechanisms of linear glassy polymers so here just a few studies will be reviewed.

We begin by looking at polymer melts and equilibrium configura-



rations. Polymer melts were modeled using amorphous cell simulations for polypropylene [70,71,82] and polycarbonates [115]. These models do not contain any thermal fluctuations and are limited to static properties. Many simulations performed restrict the motion of polymer chains to a defined lattice [94,116–120]. These methods and others could not correctly capture neutron scattering data or diffusion Vogel–Fulcher [121] behavior. Theodorou and Suter [82] examined the relaxed configuration of amorphous glassy polymers. They showed that atomistic models effectively reproduced the cohesive energy and Hildebrand solubility parameter [82] from experiments. They were also able to show that long range order did not develop in the amorphous structure.

Kremer and Grest [122–124] modeled the consequence of entanglements using MD of linear polymer melts. They showed that at a critical length of chains entanglements became present but below that point chains were not long enough to become constrained. These simulations also showed that the Rouse model [117] described the response of short chains well, but for longer chains the reptation model [117] was relevant. Brown and Clark [72] also examined amorphous glassy polymers but focused on the effect of temperature on the stress-strain behavior. They were able to predict the glass transition temperature,  $T_g$ . Brown and Clark's simulations showed that below  $T_g$  the polymer initially deformed elastically with a clear yield point followed by plastic flow. Above  $T_g$  the simulations showed a viscoelastic behavior. Brown and Clark [72] also made it very clear that atomistic simulations do not always result in the correct polymer response for a given property, especially at low temperatures ( $T < T_g$ ), primarily due to MD time scales, but qualitative comparisons are possible [72]. One property of polyethylene that is very difficult to model in atomistic is the presence of a crystalline structure, which can greatly affect the polymer's mechanical response. Kavassalis and Sundararajan [125] were able to show that crystalline phases can be created from single PE chains due to an energetic collapse of the chain. The crystalline structures are lamellar in nature and the formation is driven by the long range interaction forces between chain segments. Another aspect of polymers that should be considered beyond crystallinity is the presence of chemical cross-links. One example for developing cross-links is described by Duerig et al. [73] in which cross-linking sites are added to chains. When two cross-links are within a given distance, they are chemically linked and the chains are effectively constrained. By introducing cross-links, MD models are getting closer and closer to the actual polymer atomic structure. Further advances to the MD modeling included the introduction of a different interaction type for terminating methyl groups of PE chains [76]. To this point, there is no distinction between the potentials used to describe internal and chain terminating united atoms or beads. Since the chain ends are very important for chain migration and reptation due to the presence of free volume at chain ends, the ends should have a potential that captures the difference.

Bergström and Boyce [126] modeled a polymer network and tracked the orientation of chains to determine which energy components, bond, angle, torsion, or nonbonded, dominated the deformation. They showed that bond lengths and angles changed little throughout the deformation. The energies associated with the dihedral angle and nonbonded interactions dominated the mechanical response of the material. These simulations further showed that chains tended to align in the direction of loading with local ordering. Along with determining the critical energy components for the deformation, Bergström and Boyce [126] compared the elastic results from the MD to a network of eight chains that are aligned along the diagonals of a unit cell. Making this connection between bulk MD and an eight-chain model is an important step in linking length scales using models that are not as computationally intensive as MD simulations. Capaldi et al. [127] also performed several simulations showing that united atom methods can effectively capture the qualitative stress-strain response of poly-

mer glasses of PE type. They further showed that changes in the torsional conformation are the key deformation mechanism prior to yield. Expanding upon the idea of chain alignment, Lavine et al. [74] used stretching as a method to produce a semicrystalline structure. Upon unloading of PE, the simulations show that crystalline structures are stable. The formation of crystalline regions is enhanced by pre-orienting the chains. Yashiro et al. [128] showed chain alignment for polymers under tension and examined the entanglement structure of the chain network. Entanglements will be an important aspect of the multiscale modeling focus. Entanglements and their density determine the critical elastic chain segment length. It is clear from the above studies that MD is a vital tool in determining many of the deformation mechanisms at the atomistic level that control macroscale response.

**3.4 Impact of MD on Multiscale Models.** For the MD simulation results to have an impact on the next higher length scale, the bridge between the two scales must be clear. For example, Valavala et al. [129,130] effectively developed a continuum level hyperelastic model that incorporates the results of molecular dynamics simulations. The models by Valavala et al. [129,130] establish the upper and lower bounds for the elastic properties of polycarbonate-type polymers and validate that the elastic response of several microstates fall between these limits. The elastic responses are then inputted into the continuum models. These specific methods are limited to glassy polymers in the elastic regime but the ideas show that links between MD and coarse-graining are effective methods for finding microscale properties that can be implanted into continuum models.

Similar research to that of Valavala et al. [129,130] focused on the plastic deformation of materials at the atomistic level. Shenogin and Ozisik [131] performed MD simulations to study local plastic shear transformations (PSTs), which are the primary mechanisms for plastic deformation in glassy polymers. In this case atomistic simulations were performed to determine the size and shape of PSTs, which are then passed to a continuum type model. Other aspects of the polymer that could prove to be useful at higher length scales included the finding that localized shear occurred around atoms that have a high mobility but not necessarily a low density. While these structure-property methods show that it is possible to pass information directly from atomistics to the continuum, not all information can be captured by MD. Due to the limited amount of time that a MD simulation can model, not all deformation mechanisms are in operation, namely, reptation and chain migration. Reptation and chain sliding are believed to control the viscoelastic/plastic properties of the material. Furthermore, care must be taken when correlating the results from MD to higher length scales, in particular, when defining a representative volume element (RVE) for the system. Many of the properties found using MD simulations are dependent on the simulation size, which ultimately defines the RVE of the model [130].

## 4 Macroscale Methods

This section reviews different material models formulated at the macroscale using continuum mechanics principles, giving particular emphasis to models for amorphous polymers. The presentation proceeds by describing the large deformation kinematics and thermodynamics framework used to formulate the constitutive equations in the context of the finite element method (FEM), which allows for numerical simulations. Section 4.4 comprises a literature review of different material models used to describe the mechanical behavior of amorphous polymers and a discussion on the ability of numerical models based on internal state variables to bridge various length scales together.

**4.1 The Continuum Mechanics Approach.** At the microscopic level, polymers are viewed as a discontinuous atomic structure characterized by molecules and large gaps between them. Theories such as quantum, molecular, and atomistic theories (described above) consider a discrete structure of matter. At the mac-

rosopic scale, such theories are too computationally expensive for use in solving engineering boundary value problems. However, the research concerning polymeric materials is constantly growing driven by new engineering applications. Therefore, the development of multiscale modeling based on the bridging of the micromechanisms from lower to higher length scales is indispensable for predicting with accuracy the mechanical behavior of material under complex loading.

**4.1.1 Kinematics.** Polymeric materials are characterized by their mechanical properties during large deformations, which include large stretching and/or rotations. As such, large deformation kinematics needs a consistent formulation to follow the material deformation in space and time.

Macroscopic systems can be generally described successfully using a continuum theory. Continuum theories are based on the fundamental assumption that a body, denoted by  $B_0$ , can be defined by a continuous distribution of matter in space and time. The body is viewed as being a composition of continuum particles or material points, in which the material points represent a set of a large number of molecules.

In standard continuum mechanics form, we let  $X$  represent an arbitrary material point in  $B_0$  (essentially, a body is identified within a space with a fixed reference configuration). The motion of  $B$  is described through the mapping  $x=y(X,t)$  via a deformation gradient ( $\mathbf{F}$ ), velocity ( $v$ ), and velocity gradient ( $\mathbf{I}$ ) by the following:

$$\mathbf{F} = \nabla y, \quad v = \dot{y}, \quad \mathbf{I} = \text{grad } v = \dot{\mathbf{F}}\mathbf{F}^{-1} \quad (17)$$

An essential kinematical ingredient of elastoviscoplastic constitutive models for amorphous glassy polymers is the classical Kröner [132] and Lee [133] multiplicative decomposition of the deformation gradient  $\mathbf{F}$  into elastic and plastic (inelastic) components,

$$\mathbf{F} = \mathbf{F}^e \mathbf{F}^p, \quad J = \det \mathbf{F} = J^e J^p, \quad J^e = \det \mathbf{F}^e, \quad J^p = \det \mathbf{F}^p \quad (18)$$

As described by Anand and Gurtin [134] for polymeric materials,  $\mathbf{F}^e$  represents the elastic part due to “elastic mechanisms,” such as stretching and rotation of the intermolecular structure in polymeric material.  $\mathbf{F}^p$  represents the plastic part due to “plastic mechanisms,” such as permanent stretching and rotation due to the relative slippage of molecular chains in polymers. The decomposition (18) suggests that there exists an intermediate configuration between the underformed  $B_0$  and the current  $B$  configuration, which is denoted here by  $\bar{B}$ . Hypothetically,  $\bar{B}$  is obtained from  $B$  by unloading through  $\mathbf{F}^{e-1}$  to a zero stress state (a relaxed configuration).

Using Eqs. (17) and (18), the velocity gradient  $\mathbf{I}$  can be written as

$$\mathbf{I} = \mathbf{I}^e + \mathbf{F}^e \bar{\mathbf{L}}^p \mathbf{F}^{e-1} \quad (19)$$

with

$$\mathbf{I}^e = \dot{\mathbf{F}}^e \mathbf{F}^{e-1}, \quad \bar{\mathbf{L}}^p = \dot{\mathbf{F}}^p \mathbf{F}^{p-1} \quad (20)$$

$\mathbf{I}^e$  and  $\bar{\mathbf{L}}^p$  can be decomposed into their symmetric and skew parts, i.e.,  $\mathbf{I}^e = \mathbf{d}^e + \mathbf{w}^e$  and  $\bar{\mathbf{L}}^p = \bar{\mathbf{D}}^p + \bar{\mathbf{W}}^p$ . Two main assumptions can be made concerning the plastic flow: (i) the flow is incompressible, inducing  $\det \mathbf{F}^p = 1$  and  $\text{tr } \bar{\mathbf{L}}^p = 0$ , and (ii) the flow is irrotational, inducing  $\bar{\mathbf{W}}^p = \mathbf{0}$  [135,136] and then  $\bar{\mathbf{L}}^p = \bar{\mathbf{D}}^p$ . This last assumption has been mainly used to simplify the equations and is not based on experimental observations or molecular simulations.

The Cauchy stress [137] can be written as

$$\boldsymbol{\sigma} = \mathbf{J}^{-1} \boldsymbol{\tau} = \mathbf{J}^{-1} \mathbf{F} \mathbf{S} \mathbf{F}^T \quad (21)$$

where  $\boldsymbol{\tau}$  is the Kirchhoff stress [137], and  $\mathbf{S}$  is the corresponding second Piola–Kirchhoff stress [137] expressed in configuration  $B_0$ .

**4.1.2 Balance Principles of Continuum Mechanics.** The balance laws of continuum mechanics are essential to set the equations required to solve an initial boundary value of a thermomechanical problem. In this section, we briefly recall the fundamental balance principles of continuum mechanics, i.e., the conservation of mass, the momentum balance principles, balance of energy, and entropy inequality principle (see Ref. [137] for a detailed review). They are applicable to any material and must be satisfied at any time.

The balance of mass states that the total mass of a closed system remains constant, i.e.,

$$\dot{\rho} + \rho \text{div}(\mathbf{v}) = 0 \quad (22)$$

where  $\rho$  is the spatial mass density. The balance of linear momentum states that the time rate of linear momentum of a volume is equal to the sum of the force acting on the body and allows the deduction in Cauchy’s first equation of motion, i.e.,

$$\text{div } \boldsymbol{\sigma} + \mathbf{b} = \rho \dot{\mathbf{v}} \quad (23)$$

The balance of angular momentum states that the time derivative of the moment of linear momentum is required to be equal to the sum of the moments of the forces acting on the body acting on the same point. The balance of angular momentum results in the symmetry of the Cauchy stress tensor  $\boldsymbol{\sigma}$ , i.e.,

$$\boldsymbol{\sigma} = \boldsymbol{\sigma}^T \quad (24)$$

The balance of energy (first law of thermodynamics) states that the rate of work performed on the continuum body, defined by the sum of the rate of internal work  $P_{\text{int}}(t)$  and the rate of thermal work  $Q(t)$  is equal to the rate of internal energy  $\epsilon(t)$ . The first law of thermodynamics written in configuration  $B$  is given by

$$P_{\text{int}}(t) + Q(t) = \frac{D}{Dt} \epsilon(t) \quad (25)$$

with

$$P_{\text{int}}(t) = \int_B \boldsymbol{\sigma} : \mathbf{I} dv, \quad Q(t) = \int_B (-\nabla \cdot \mathbf{q} + r_v) dv, \quad \epsilon(t) = \int_B e_v dv \quad (26)$$

where  $e_v$ ,  $q$ , and  $r_v$  are, respectively, the specific internal energy (per unit volume), the heat flux per unit area, and the heat source per unit volume expressed in the configuration  $B$ .

The first law of thermodynamics governs the energy transfer in the thermodynamic system but gives no statement on the direction of the energy transfer like the second law of thermodynamic, which dictates the direction of energy transfer. The second law of thermodynamics introduces the concept of entropy. The entropy can be viewed as a measure of microscopic randomness and disorder [138]. The second law of thermodynamics states that the total production of entropy per unit time is always positive. The entropy inequality principle can also be written in the form commonly referred to as the Clausius–Duhem inequality [137],

$$\dot{\eta}_v - \frac{r_v}{\theta} + \frac{1}{\theta} \nabla \cdot \mathbf{q} - \frac{1}{\theta^2} \mathbf{q} \cdot \nabla \theta \geq 0 \quad (27)$$

where  $\eta_v$  is the specific internal entropy (per unit volume), and  $\theta$  is the absolute temperature. The Helmholtz free energy is introduced through the Legendre transformation,

$$\psi_v = e_v - \theta \eta_v \quad (28)$$

By substituting Eq. (25) into the Clausius–Duhem inequality (Eq. (27)), and using Eqs. (26) and (28) lead to the equation formulated in terms of Helmholtz free energy:

$$\boldsymbol{\sigma} : \mathbf{I} - \dot{\psi} - \dot{\theta} \eta - \frac{1}{\theta} \mathbf{q} \cdot \nabla \theta \geq 0 \quad (29)$$



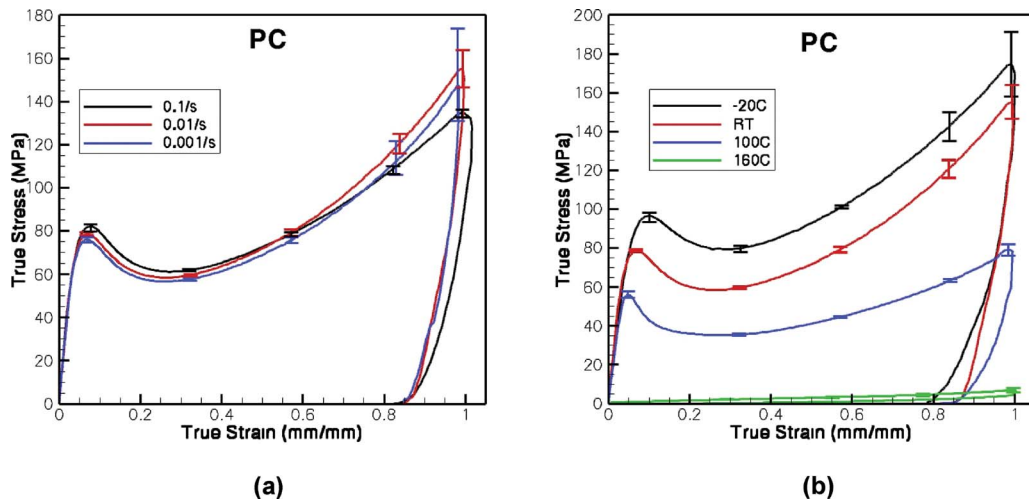


**Fig. 3 Mechanical response of PC under compression: (a) for different strain rates at room temperature (RT) and (b) for different temperatures at an applied strain rate of 0.01/s.**

**4.1.3 Constitutive Relations.** The study of inelastic materials such as polymeric materials gave rise to the development of new constitutive models based on internal state variables. In contrast to variables  $\mathbf{F}$ ,  $\mathbf{C}$  (Cauchy–Green tensor), or  $\theta$ , which are external observable variables, internal variables also known as hidden variables represent microstructure, defects, grains, and items embedded within the material. A general framework based on a thermodynamic approach with internal state variables has been developed and used to predict the mechanical properties of metals and polymers [139–143].

Assuming that the Helmholtz free energy is dependent on observable variable  $\mathbf{C}$  and a set of additional internal variables  $\xi_\alpha$ ,  $\alpha = 1, \dots, n$ , we can write the following:

$$\psi = \psi(\mathbf{C}, \xi_1, \xi_2, \dots, \xi_n) \quad (30)$$

where  $\xi_i$  are the internal state variables. Equation (29) serves as a major mathematical restriction on the constitutive equations governing the evolution of internal variables and heat conduction. Introducing Eq. (30) in Eq. (29) and using the classical arguments [139], the different equations of state are obtained for the Cauchy stress and the thermodynamic forces  $\mathbf{A}_\alpha$  associated with the internal variables  $\xi_\alpha$ .

$$\boldsymbol{\sigma} = \mathbf{J}^{-1} \mathbf{F} \left( 2 \frac{\partial \psi}{\partial \mathbf{C}} \right) \mathbf{F}^T, \quad \mathbf{A}_\alpha = \frac{\partial \psi}{\partial \xi_\alpha} \quad (31)$$

**4.2 FEM.** The continuum mechanics theory, described in Sec. 4.1, is mainly based on differential equations describing the evolution of the material behavior in space and time. An engineering tool has been developed to employ these equations in the context of complex boundary conditions. This tool is called the FEM, which is a general numerical method for finding approximate solutions of partial differential equations. Material constitutive equations need to be implemented in finite element codes to be used in structural computations. FEM uses spatially discretized domains, which allows capturing complex geometries and spatial discontinuities. It also allows incorporating nonlinear constitutive equations to take account of the complex mechanical properties of materials. The global system of equations, taking into account the boundary conditions, is then solved to calculate the state variables. Details can be found in books especially devoted to FEM [144–146]. FEM has been incorporated in some commercial software packages and open source codes (e.g., ANSYS, LS-DYNA, ABAQUS, and ZEBULON to name a few) and is widely used in industry as a tool to predict the mechanical properties of polymers.

**4.3 Constitutive Models for Amorphous Polymers.** Polymeric materials are used in an increasing number of products ranging from simple consumer goods to advanced aerospace structures. The research concerning polymeric materials is constantly growing because of the demands for lighter and impact resistance materials. Components made in amorphous polymers are used in automotive applications for their compatibilities with aggressive automotive fluids, their exceptional strength at high temperatures, and their excellent resistance to creep, wear, and chemicals including organic solvents. Polymers exhibit a rich variety of material behavior, due to their particular microstructure (long molecular chains). Also, their macroscopic material behavior is strongly temperature, pressure, and time dependent. A number of constitutive models have been developed and implemented in FEM codes in an effort to solve complex engineering problems with polymers. However, the improvement of constitutive models capturing the complicated mechanical properties of polymers is always challenging and has importance for the design of structural components. This section is focused on an overview of constitutive models developed for polymers with a particular emphasis on amorphous glassy polymer models.

In Fig. 3, the mechanical response of PC under compression for different strain rates and temperatures is depicted. As noted from Fig. 3(a), all the curves show the expected features of the mechanical response for amorphous glassy polymers at temperatures below the glass transition temperature: an initial linear elastic response followed by a nonlinear transition curve to global yield, and then strain softening followed by strain hardening. The stress response also exhibits an increased yield peak value with increasing applied strain rate. The effect of temperature on the mechanical behavior is presented Fig. 3(b). As displayed by Fig. 3(b), the yield stress, the initial Young modulus, and the hardening decreased as the temperature increased. We can also note that for temperatures above  $T_g$  (reported as about  $150^\circ\text{C}$  for PC in the literature), the material is in a rubbery regime.

In the literature, several theoretical models have been established to evaluate the complex nature of glassy polymers with the main purpose of capturing their mechanical behavior. These continuum models can be grouped into two major categories: phenomenological and physically based models.

The phenomenological models attempt to describe the mechanical response of the material with few considerations of the internal structure. Models, initially developed for metals, were used to reproduce the mechanical properties of polymers. For instance, Van der Sluis et al. [147] predicted the nonlinear behavior of

polycarbonate by using the viscoplastic overstress model of Perzyna [148]. In the same way, a viscoplasticity theory based on overstress (VBO) developed by Krempl [149,150] was used to describe the behavior of highly crystalline polymers such as Polyamide 66 or high-density polyethylene [151–153], characterized by a mechanical behavior close from those of metals. A second class of phenomenological models based on differential equations and combining linear and nonlinear springs with dashpots has been largely used to predict the viscoelastic response of polymers [154–158]. A different approach based on non-Newtonian fluid mechanics [159] was proposed by Tervoort et al. [160] to describe the nonlinear viscoelastic behavior of glassy polymers. This model was refined to account for the softening and hardening effects on the mechanical response [161,162]. This review is not exhaustive as other phenomenological constitutive models for glassy polymers have been developed in the literature [158,163–165]. Even though these phenomenological models showed their capability to reproduce the inelastic behavior of polymers for a range of specific loading, many important structural and mechanical features were not included; hence, the modeling of history effects is typically lacking. As discussed by Anand and Ames [166], these models developed to predict macroscopic testing results will generally fail in the prediction of micromechanical testing like indentation tests. Moreover, this deficiency of not including microstructural features makes the usage of these models difficult in a multiscale modeling strategy.

The purpose of the physically based models is to capture the detailed mechanical responses by including the internal microstructure of the material. Haward and Thackray [167] pioneered the material modeling of glassy polymers by the use of yield/flow model (based on Eyring theory [168]) combined with rubbery hyperelastic model (three-chain model of James and Guth [169]). This idea was extended by Boyce et al. [170] to a three-dimensional model using the theory of Argon [171] to model the flow stress and the three-chain model [169] to take account of the stress hardening behavior at large strains.

Regarding the flow stress, three main theories can be found in the literature. The first model used to describe the rate-dependent plastic flow was developed by Eyring [168]. Eyring's theory based on "transition state" theory considers the idea that one molecule transitioned from a particular state or potential energy to another by overcoming an energy barrier. Another widely accepted theory was developed by Robertson [172]. In the Robertson model, the plasticity was attributed to a thermally activated transition of molecular structural states from flexed to extended configurations by rotation of chain segments. Argon [171] presented an alternate theory (molecular double-kink theory) based on a thermally activated molecular motion where the resistance to the plastic flow was attributed to intermolecular forces due to the alignment of previously kinked chains in the direction of the straining. All three theories proved their ability to predict the rate and temperature dependent yield stress of various amorphous polymers. However, they are unable to capture the yield stress evolution at low temperature and moderate to high rates of deformation. Later, Ree and Eyring [173,174] advanced a theory based on multiple rate-activated processes, and Fotheringham and Cherry [175,176] developed a theory based on complex "cooperative" activation process. In both cases, they have shown their abilities to capture the yield stress behavior across a wide range of temperatures and/or strain rates.

Regarding the stress hardening in the amorphous glassy polymers, all of the proposed models fall into one of the two schools of thought: the continuum approach [177–180] and the statistical approach. Regarding the statistical approach, we can mention the three-chain model from James and Guth [169], the eight-chain model from Arruda and Boyce [181], and the works of Wu and van der Giessen [182], Elias-Zuniga and Beatty [183], and Miehe et al. [184]. From a multiscale point of view, the statistical ap-

proach is more appropriate to capture the microstructural evolution. This approach derives stress-strain properties from an idealized model of its molecular structure.

More degrees of freedom can be added to the continuum models [166,185,186] to account for micromechanisms in order to capture the mechanical properties of polymers through a range of temperatures (below and above the glass transition temperature) and strain rates (from low to high strain rates). For instance, Mulliken and Boyce [185] proposed a micromechanical model for the amorphous polycarbonate based on the  $\alpha$ - and  $\beta$ -mechanisms representing the rotation of main-chain segments and phenyl group in order to describe the yield strength of the material. The use of MD simulations opened an avenue to provide understanding of the various micromechanism evolutions and their associated connectedness to the macroscale mechanical response. Thus, Capaldi et al. [127] showed the connection between the free volume evolution and the macroscale softening. This dependence has been used in continuum models to improve the mechanical response of amorphous glassy polymers [136,187,188]. As discussed in more detail in Sec. 4.4, Shepherd et al. [83,84] developed an interesting ISV model based on a hierarchical multiscale strategy able to predict the evolution of polymer morphology such as entanglement and crystallization and reproduce the mechanical behavior of semicrystalline polymers over a range of temperatures and strain rates. Although most of these models capture accurately the mechanical properties of polymers for simple loading cases, they typically cannot capture the mechanical response when submitted to complex cyclic loading cases. These results show that some important micromechanisms are not yet completely understood and described in the polymeric models. Efforts need to be done to continue building the bridging between the different length scales.

**4.4 Multiscale Strategy Using Internal State Variables Formulation.** ISV is a constitutive modeling theory that can admit physical microstructural features. A discussion on the use of internal state variables models coupled with hierarchical multiscale modeling as a challenging solution is presented in this section. ISV (see Ref. [189]) constitutive models are based on the use of thermodynamical constraints and can be physically based on microstructure-property relations. ISVs are differential variables and are functions of observable variables such as temperature, strain rate, and stress state. The ISV method is an effective method of hierarchical modeling in which numerical methods are independently run at various length scales and then a bridging methodology is adopted. It is a top-down approach, meaning the ISVs exist at the macroscale but reach down to various subscales to receive pertinent information. ISV applications have been extensively studied in solid mechanics, but ISV theory has probably had its greatest impact on metals. Recently, microstructure-property relations have been included in ISVs to capture history effects of cast aluminum and wrought aluminum [3,190–192]. The hierarchical multiscale methodology has been employed for monotonic and fatigue loads [193,194]. Examples of multiscale hierarchical methods have been demonstrated by Horstemeyer and co-workers [195–197]. For these examples, experiments were used to validate the modeling at a particular scale, and then the pertinent effects, not all of the causes, were brought up into the macroscale level. In the multiscale work of Horstemeyer and co-workers [195–197], ISVs were used as a top-down approach to bring into the macroscale the pertinent nanoscale, microscale, and mesoscale phenomena.

Although metals have enjoyed a rich history of ISV usage, the application to polymers has not been as prevalent. The complexities of polymers are different than metals, but the methodology of embedding mechanisms into the ISV framework that are constrained by thermodynamics is the same. Arruda et al. [181] developed an ISV formulation for evolving anisotropic viscoelastic polymers based on the previous viscoplastic formulations. During processing glassy polymers produce highly anisotropic polymer components as a result of the massive reorientation of molecular

chains during the large strain deformations. Using material properties from initially isotropic material, simulations were shown to capture the important aspects of the large strain anisotropic response including flow strengths, strain hardening characteristics, cross-sectional deformation patterns, and limiting extensibilities. Later, others developed ISV theories for polymers. Schapery [198] developed an ISV formalism for nonequilibrium thermodynamics, strain rate sensitive, viscoelastic fracture mechanics that accounted for effects of viscoelasticity, viscoplasticity, growing damage, and aging. Within this research effort, Schapery [198] analyzed the isotropic and anisotropic aspects of the ISV formalism. Yoon and Allen [199] introduced a cohesive fracture model into an ISV formulation for nonlinear viscoelasticity materials. Also, Wei and Chen [200] proposed an ISV model that extended the network theory of rubber elasticity with viscosity. Ghorbel [201] also proposed a viscoplastic ISV formulation to predict the mechanical behavior of polymer by changing the yield function capturing the plastic flow to include the first three invariants of stress and therefore take into account the pressure dependence and strong deviatoric interactions. Finally, Anand et al. [202] and Ames et al. [203] recently developed a thermomechanical model for amorphous polymers based on internal state variables representing the important aspect of the microstructure resistance to plastic flow. This model predicted the mechanical behavior of amorphous polymers for various types of testing (compression, reversed torsion, isothermal forging, and impact test).

However, most of these models assume phenomenological evolution equations for their internal state variables and thus do not consider a hierarchical multiscale strategy. A review of hierarchical multiscale modeling in polymers can be found in Refs. [100,204,205]. These papers discussed new methods and algorithms that can be used for predicting thermal, mechanical, and rheological properties of polymers. Shepherd et al. [83,84] developed an interesting multiscale modeling strategy for semicrystalline polymers tracking the evolution of entanglement density through MD simulations during thermomechanical deformations and then passing the evolution equations from nanoscale structures to an ISV model. They showed that an ISV material model that takes into account the atomistic structure behavior of the material accurately reproduces over a range of strain rates and temperatures the mechanical behavior and the evolution of crystallinity and orientation of semicrystalline polymers. Their work emphasizes the impact that could have the development of multiscale modeling in the way to synthesize and optimize polymer morphology for specific applications.

Regarding amorphous polymers, we know that free volume, intramolecular (chains rotation) and intermolecular (Van der Waals forces) resistances, entanglement number density, crystallization, and crystal number density drive the mechanical features of polymer at the macroscale. Questions to consider in modeling this class of polymers are the following: Are these mechanisms time, temperature, or stress state dependent? Can they be quantified? What are the damage mechanisms and their associated evolution rates from nanoscale or microscale? With the evolution of computer simulations, are we now able to model a realistic microstructure of an amorphous polymer? The answer is probably "no." But we are now able to model idealized microstructures of polymers and track the main micromechanisms (such as entanglements and free volume evolution) through different length scales. Efforts need to focus on the understanding of the nonlinear mechanical behavior of polymers to resolve path history dependence in order to solve complex engineering boundary value problems.

## 5 Summary

The development of new material systems that are safe, ultralightweight, cost-effective, and manufacturable is at the forefront of designing industrial components. The potential for polymer based structural components is now becoming realized, but challenges still exist. The challenges of creating an effective com-

ponent often require a rigorous description of material behavior from the nano- to macroscale. Having a predictive physics-based model is one key method of facing these challenges. In addition, testing in terms of model exploration, model calibration, and model validation needs to be continued with an eye for structure-property quantification.

In this paper, we reviewed hierarchical multiscale methods focusing on the mechanical behavior of amorphous polymers. Different methods can be used for this purpose: QM, MD, and CM. QM uses different methods including DFT to capture interatomic and conformation energies [47–59]. QM predicts energies quite well for systems on the order of a few hundred atoms. For larger systems of atoms, the computational time becomes unreasonable resulting in the need for other modeling techniques. The information calculated from QM assists in the development of potentials for larger MD and bead-spring (coarse-grained) simulations [59–65]. MD and bead-spring methods model molecules and chains on the order of millions of atoms for a few nanoseconds. MD simulations capture elastic and viscous properties of the material and determine the deformation mechanisms controlling the motion [74,82–84,126–128]. Since there are significant differences in time between the many deformation mechanisms including conformation changes and reptation, the time scale of MD is not always sufficient. Time scales can be increased by orders of magnitude using MC [96,106] and hyperdynamics [107,108], but the lengths are still limited to millions of atoms. One goal of the MD simulations is to develop evolution equations and energetic relations for each mechanism to be passed to CM simulations [83,84]. This link still requires a significant amount of research to move away from phenomenological evolution equations. CM simulations remove the atomistic details of the problem and are used to solve the largest size problems. Generally the evolution equations used in continuum models are phenomenological and lack physical meaning [166]. For a rigorous and complete multiscale strategy, the nanoscale properties of importance should be present at all length and time scales. Multiscale modeling has had a great impact on metals (ordered structure) relative to amorphous polymers, but the work done on metals can only be a guide for the work in expanding the multiscale modeling of polymers [83,84,100,204,205] as the mechanisms related to the time and length scales are different.

The primary challenge of a multiscale model for polymers is the development of a hierarchical physically validated and numerically verified suite of multiscale theoretical/computational models for materials. These models should provide a fundamental understanding to direct and control matter starting at the quantum level to achieve novel physical and thermomechanical properties. With increasing computational power and the associated software tools, the ability to quantify the structure-property relations of polymers at different length scales is still far from being achieved. Yet, the current works reviewed here show that many are facing the challenges created by this vast problem. A functional hierarchical multiscale model would be an efficient and effective design tool for structural components that will ultimately save industry time and money while increasing efficiency and safety for consumers.

## Acknowledgment

The authors would like to thank the Center for Advanced Vehicular Systems (CAVS) at Mississippi State University for funding this effort. The authors would also like to thank the Army TARDEC group for their support.

## References

- [1] De Pablo, J. J., and Curtin, W. A., 2007, "Multiscale Modeling in Advanced Materials Research," *MRS Bull.*, **32**(11), pp. 905–911.
- [2] Horstemeyer, M. F., 2001, "From Atoms to Autos: Part 1 Monotonic Modeling," Sandia National Laboratories, Report No. SAND2001-8662.
- [3] Horstemeyer, M. F., and Wang, P., 2003, "Cradle-to-Grave Simulation-Based Design Incorporating Multiscale Microstructure-Property Modeling: Reinviso-



- rating Design With Science," J. Comput. Aided Mater. Des., **10**, pp. 13–34.
- [4] Tadmor, E. B., 1996, "The Quasicontinuum Method," Ph.D. thesis, Brown University, Providence, RI.
- [5] Tadmor, E. B., Ortiz, M., and Phillips, R., 1996, "Quasicontinuum Analysis of Defects in Solids," *Philos. Mag. A*, **73**, pp. 1529–1563.
- [6] Shilkrot, L. E., Curtin, W. A., and Miller, R. E., 2002, "A Coupled Atomistic/Continuum Model of Defects in Solids," *J. Mech. Phys. Solids*, **50**, pp. 2085–2106.
- [7] Campbell, C. E., and Olson, G. B., 2000, "Systems Design of High Performance Stainless Steels I. Conceptual and Computational Design," *J. Comput. Aided Mater. Des.*, **7**, pp. 145–170.
- [8] Groh, S., Marin, E., Horstemeyer, M., and Zbib, H. M., 2009, "Multiscale Modeling of the Plasticity in an Aluminium Single Crystal," *Int. J. Plast.*, **25**, pp. 1456–1473.
- [9] Flory, P. J., 1989, *Statistical Mechanics of Chain Molecules*, Interscience, New York.
- [10] Binder, K., 1995, *Monte Carlo and Molecular Dynamics Simulations in Polymer Science*, Oxford University Press, New York.
- [11] Christopher, J. C., 2002, *Essentials of Computational Chemistry, Theories and Model*, Wiley, New York.
- [12] Levine, I. N., 1991, *Quantum Chemistry*, Prentice-Hall, Englewood Cliffs, NJ, pp. 455–544.
- [13] Szabo, A., and Ostlund, N. S., 1996, *Modern Quantum Chemistry*, Dover, Mineola, NY.
- [14] Leininger, M. L., Allen, W. D., Schaefer, H. F., and Sherrill, C. D., 2000, "Is Møller-Plesset Perturbation Theory a Convergent *ab initio* Method?," *J. Chem. Phys.*, **112**(21), pp. 9213–9222.
- [15] Hurley, A. C., 1976, *Electronic Correlation in Small Molecules*, Academic, New York.
- [16] Bartlett, R. J., 1981, "Many Body Perturbation Theory and Coupled Cluster Theory for Electron Correlation in Molecules," *Annu. Rev. Phys. Chem.*, **32**, pp. 359–401.
- [17] Knowles, P. J., and Werner, H. J., 1985, "An Efficient Second-Order MC SCF Method for Long Configuration Expansions," *Chem. Phys. Lett.*, **115**, pp. 259–267.
- [18] Werner, H. J., and Knowles, P. J., 1985, "A Second Order Multiconfiguration SCF Procedure With Optimum Convergence," *J. Chem. Phys.*, **82**, pp. 5053–5063.
- [19] Pople, J., and Beveridge, D., 1970, *Approximate Molecular Orbital Theory*, McGraw-Hill, New York.
- [20] Pople, J. A., and Segal, G. A., 1965, "Approximate Self-Consistent Molecular Orbital Theory. II. Calculations With Complete Neglect of Differential Overlap," *J. Chem. Phys.*, **43**, pp. S136–S151.
- [21] Pople, J. A., Santry, D. P., and Segal, G. A., 1965, "Approximate Self-Consistent Molecular Orbital Theory. I. Invariant Procedures," *J. Chem. Phys.*, **43**, pp. 129–135.
- [22] Pople, J. A., and Segal, G. A., 1966, "Approximate Self-Consistent Molecular Orbital Theory. III. CNDO Results for AB<sub>2</sub> and AB<sub>3</sub> Systems," *J. Chem. Phys.*, **44**, pp. 3289–3296.
- [23] Gordon, M. S., and Pople, J. A., 1968, "Approximate Self-Consistent Molecular-Orbital Theory. VI. INDO Calculated Equilibrium Geometries," *J. Chem. Phys.*, **49**, pp. 4643–4650.
- [24] Dewar, M. J. S., and Thiel, W., 1977, "Ground States of Molecules. 38. The MNDO Method. Approximations and Parameters," *J. Am. Chem. Soc.*, **99**, pp. 4899–4907.
- [25] Bingham, R. C., Dewar, M. J. S., and Lo, D. H., 1975, "Ground States of Molecules. XXV. MINDO/3. Improved Version of the MINDO Semiempirical SCF-MO Method," *J. Am. Chem. Soc.*, **97**, pp. 1285–1293.
- [26] Dewar, M. J. S., Zoebisch, E. G., Healy, E. F., and Stewart, J. J. P., 1985, "Development and Use of Quantum Mechanical Molecular Models. 76. AM1: A New General Purpose Quantum Mechanical Molecular Model," *J. Am. Chem. Soc.*, **107**, pp. 3902–3909.
- [27] Dreizler, R. M., and Gross, E. K. U., 1990, *Density Functional Theory*, Springer, Berlin.
- [28] Parr, R. G., and Yang, W., 1989, *Density Functional Theory of Atoms and Molecules*, Oxford University Press, New York.
- [29] Hohenberg, P., and Kohn, W., 1964, "In Homogeneous Electron Gas," *Phys. Rev.*, **136**, pp. B864–B871.
- [30] Kohn, W., and Sham, L. J., 1965, "Self-Consistent Equations Including Exchange and Correlation Effects," *Phys. Rev.*, **140**, pp. A1133–A1138.
- [31] Jones, R. O., and Gunnarsson, O., 1989, "The Density Functional Formalism, Its Applications and Prospects," *Rev. Mod. Phys.*, **61**, pp. 689–746.
- [32] Perdew, J. P., 1991, *Electronic Structure of Solids*, P. Ziesche and H. Eschrig, eds., Akademie, Berlin, p. 11.
- [33] Fulde, P., 1993, *Electron Correlations in Molecules and Solids*, Springer, Berlin.
- [34] Perdew, J. P., Burke, K., and Wang, Y., 1996, "Generalized Gradient Approximation for the Exchange-Correlation Hole of a Many-Electron System," *Phys. Rev. B*, **54**, pp. 16533–16539.
- [35] Perdew, J. P., and Zunger, A., 1981, "Self-Interaction Correction to Density-Functional Approximations for Many Electron Systems," *Phys. Rev. B*, **23**, pp. 5048–5079.
- [36] Tao, J., Perdew, J. P., Staroverov, V. N., and Scuseria, G. E., 2003, "Climbing the Density Functional Ladder: Nonempirical Meta-Generalized Gradient Approximation Designed for Molecules And Solids," *Phys. Rev. Lett.*, **91**, p. 146401.
- [37] Mattsson, A. E., Schultz, P. A., Desjarlais, M. P., Mattsson, T. R., and Leung, K., 2005, "Designing Meaningful Density Functional Theory Calculations in Materials Science—A Primer," *Modell. Simul. Mater. Sci. Eng.*, **13**, pp. R1–R31.
- [38] Adamo, C., and Barone, V., 1998, "Exchange Functional With Improved Long-Range Behavior and Adiabatic Connection Methods Without Adjustable Parameters: The mPW and mPW1PW Models," *J. Chem. Phys.*, **108**, pp. 664–675.
- [39] Becke, A. D., 1993, "Density-Functional Thermochemistry. III. The Role of Exact Exchange," *J. Chem. Phys.*, **98**, pp. 5648–5652.
- [40] Filatov, M., and Thiel, W., 1997, "A New Gradient-Corrected Exchange-Correlation Density Functional," *Mol. Phys.*, **91**, pp. 847–859.
- [41] Lee, C., Yang, W., and Parr, G. R., 1988, "Development of the Colle-Salvetti Correlation-Energy Formula Into a Functional of the Electron Density," *Phys. Rev. B*, **37**, pp. 785–789.
- [42] Perdew, J. P., Burke, K., and Ernzerhof, M., 1996, "Generalized Gradient Approximation Made Simple," *Phys. Rev. Lett.*, **77**, pp. 3865–3868.
- [43] Perdew, J. P., Chevary, J. A., Vosko, S. H., Jackson, K. A., Pederson, M. R., Singh, D. J., and Fiolhais, C., 1992, "Atoms, Molecules, Solids, and Surfaces: Applications of the Generalized Gradient Approximation for Exchange and Correlation," *Phys. Rev. B*, **46**, pp. 6671–6687.
- [44] Stephens, P. J., Devlin, F. J., Chabalowski, C. F., and Frisch, M. J., 1994, "Ab Initio Calculation of Vibrational Absorption and Circular Dichroism Spectra Using Density Functional Force Fields," *J. Phys. Chem.*, **98**, pp. 11623–11627.
- [45] Turkowski, V. C., and Ullrich, C. A., 2008, "Time-Dependent Density-Functional Theory for Ultrafast Interband Excitations," *Phys. Rev. B*, **77**, p. 075204.
- [46] Carter, E. A., 2008, "Challenges in Modeling Materials Properties Without Experimental Input," *Science*, **321**, pp. 800–803.
- [47] Perez, S., and Scaringe, R. P., 1987, "Crystalline Features of 4,4'-Isopropylidenediphenylbis(Phenyl Carbonate) and Conformational Analysis of the Polycarbonate of 2,2-Bis(4-Hydroxyphenyl)Propane," *Macromolecules*, **20**, pp. 68–77.
- [48] Henrichs, P. M., and Luss, H. R., 1988, "Ring Dynamics in a Crystalline Analog of Bisphenol A Polycarbonate," *Macromolecules*, **21**, pp. 860–862.
- [49] Williams, A. D., and Flory, P. J., 1968, "Analysis of the Random Configuration of the Polycarbonate of diphenylol-2,2'-propane," *J. Polym. Sci., Polym. Phys. Ed.*, **6**, pp. 1945–1952.
- [50] Tonelli, A. E., 1972, "Conformational Characteristics of Isotactic Polypropylene," *Macromolecules*, **5**, pp. 563–566.
- [51] Bicerano, J., Hayden, A., and Clark, J. H., 1988, "Intrachain Rotations in the Poly(Ester Carbonates) 1. Quantum Mechanical Calculations on the Model Molecules 2,2-Diphenylpropane, Diphenylcarbonate, and Phenyl Benzoate," *Macromolecules*, **21**, pp. 585–597.
- [52] Bicerano, J., Hayden, A., and Clark, J. H., 1988, "Intrachain Rotations in the Poly(Ester Carbonates) 2. Quantum-Mechanical Calculations on Large Model Molecules Fully Representing Each Type of Phenyl Ring Environment," *Macromolecules*, **21**, pp. 597–603.
- [53] Bernard, C., Laskowski, B. C., Do, Y., Yoon, D. Y., McLean, D., Richard, L., and Jaffe, R. L., 1988, "Chain Conformations of Polycarbonate From *ab initio* Calculations," *Macromolecules*, **21**, pp. 1629–1633.
- [54] Labrenz, D., and Schröer, W., 1991, "Conformational Analysis of Symmetric Carbonic Acid Esters by Quantum Chemical Calculations and Dielectric Measurements," *J. Mol. Struct.*, **249**, pp. 327–341.
- [55] Sun, H., Mumby, S. J., Maple, J. R., and Hagler, A. T., 1995, "Ab Initio Calculations on Small Molecule Analogs of Polycarbonates," *J. Phys. Chem.*, **99**, pp. 5873–5882.
- [56] Whitney, D. R., and Yaris, R., 1997, "Local Mechanism of Phenyl Ring-Flips in Glassy Polycarbonate," *Macromolecules*, **30**, pp. 1741–1751.
- [57] Montanari, B., Ballone, P., and Jones, R. O., 1998, "Density Functional Study of Crystalline Analogs of Polycarbonates," *Macromolecules*, **31**, pp. 7784–7790.
- [58] Montanari, B., Ballone, P., and Jones, R. O., 1998, "Density Functional Study of Molecular Crystals: Polyethylene and a Crystalline Analog of Bisphenol-A Polycarbonates," *J. Chem. Phys.*, **108**, pp. 6947–6951.
- [59] Montanari, B., Ballone, P., and Jones, R. O., 1999, "Density Functional Study of Polycarbonate. 2. Crystalline Analogs, Cyclic Oligomers, and Their Fragments," *Macromolecules*, **32**, pp. 3396–3404.
- [60] Sun, H., Mumby, S. J., Maple, J. R., and Hagler, A. T., 1994, "An Ab Initio CFF93 All-Atom Force Field for Polycarbonates," *J. Am. Chem. Soc.*, **116**, pp. 2978–2987.
- [61] Ballone, P., Montanari, B., and Jones, R. O., 1999, "Polycarbonate Simulations With a Density Functional Based Force Field," *J. Phys. Chem.*, **103**, pp. 5387–5398.
- [62] Karasawa, N., Dasgupta, S., and Goddard, W. A., III, 1991, "Mechanical Properties and Force Field Parameters for Polyethylene Crystal," *J. Phys. Chem.*, **95**, pp. 2260–2272.
- [63] Sun, H., 1998, "COMPASS: An Ab Initio Force-Field Optimized for Condensed-Phase Applications—Overview With Details on Alkane and Benzene Compounds," *J. Phys. Chem. B*, **102**, pp. 7338–7364.
- [64] van Duin, A. C. T., Dasgupta, S., Lorant, F., and Goddard, W. A., III, 2001, "ReaxFF: A Reactive Force Field for Hydrocarbons," *J. Phys. Chem. A*, **105**, pp. 9396–9409.
- [65] Dasgupta, S., Yamasaki, T., and Goddard, W. A., III, 1996, "The Hessian Biased Singular Value Decomposition Method for Optimization and Analysis of Force Fields," *J. Chem. Phys.*, **104**, pp. 2898–2920.
- [66] Verlet, L., 1967, "Computer "Experiments" on Classical Fluids. I. Thermody-

- namical Properties of Lennard-Jones Molecules," *Phys. Rev.*, **159**, pp. 98–103.
- [67] Allen, M. P., and Tildesley, D. J., 1987, *Computer Simulation of Liquids*, Oxford University Press, New York.
- [68] Nosé, S., 1984, "A Unified Formulation of the Constant Temperature Molecular Dynamics Methods," *J. Chem. Phys.*, **81**, pp. 511–519.
- [69] Hoover, W. G., 1985, "Canonical Dynamics: Equilibrium Phase-Space Distributions," *Phys. Rev. A*, **31**, pp. 1695–1697.
- [70] Theodorou, D. N., and Suter, U. W., 1986, "Atomistic Modeling of Mechanical Properties of Polymeric Glasses," *Macromolecules*, **19**, pp. 139–154.
- [71] Theodorou, D. N., and Suter, U. W., 1986, "Local Structure and the Mechanism of Response to Elastic Deformation in a Glassy Polymer," *Macromolecules*, **19**, pp. 379–387.
- [72] Brown, D., and Clark, J. H. R., 1991, "Molecular Dynamics Simulation of an Amorphous Polymer Under Tension. I. Phenomenology," *Macromolecules*, **24**, pp. 2075–2082.
- [73] Duering, E. R., Kremer, K., and Grest, G. S., 1994, "Structure and Relaxation of End-Linked Polymer Networks," *J. Chem. Phys.*, **101**, pp. 8169–8192.
- [74] Lavine, M. S., Waheed, N., and Rutledge, G. C., 2003, "Molecular Dynamics Simulation of Orientation and Crystallization of Polyethylene During Uniaxial Extension," *Polymer*, **44**, pp. 1771–1779.
- [75] Capaldi, F. M., Boyce, M. C., and Rutledge, G. C., 2004, "Molecular Response of a Glassy Polymer to Active Deformation," *Polymer*, **45**, pp. 1391–1399.
- [76] Paul, W., Binder, K., Kremer, K., and Heermann, D. W., 1991, "Structure-Property Correlation of Polymers, a Monte Carlo Approach," *Macromolecules*, **24**, pp. 6332–6334.
- [77] Tschöp, W., Kremer, K., Batoulis, J., Bürger, T., and Hahn, O., 1998, "Simulation of Polymer Melts. I. Coarse-Graining Procedure for Polycarbonates," *Acta Polym.*, **49**, pp. 61–74.
- [78] Tschöp, W., Kremer, K., Hahn, O., Batoulis, J., and Bürger, T., 1998, "Simulation of Polymer Melts. II. From Coarse-Grained Models Back to Atomistic Description," *Acta Polym.*, **49**, pp. 75–79.
- [79] Underhill, P. T., and Doyle, P. S., 2004, "On the Coarse-Graining of Polymers Into Bead-Spring Chains," *J. Non-Newtonian Fluid Mech.*, **122**, pp. 3–31.
- [80] León, S., van der Vegt, N., Delle Site, L., and Kremer, K., 2005, "Bisphenol A Polycarbonate: Entanglement Analysis From Coarse-Grained MD Simulations," *Macromolecules*, **38**, pp. 8078–8092.
- [81] Plimpton, S., 1995, "Fast Parallel Algorithms for Short-Range Molecular Dynamics," *J. Comput. Phys.*, **117**, pp. 1–19.
- [82] Theodorou, D. N., and Suter, U. W., 1985, "Detailed Molecular Structure of a Vinyl Polymer Glass," *Macromolecules*, **18**, pp. 1467–1478.
- [83] Shepherd, J. E., McDowell, D. L., and Jacob, K. I., 2006, "Modeling Morphology Evolution and Mechanical Behavior During Thermo-Mechanical Processing of Semi-Crystalline Polymers," *J. Mech. Phys. Solids*, **54**, pp. 467–489.
- [84] Shepherd, J. E., 2006, "Multiscale Modeling of the Deformation of Semi-Crystalline Polymers," Ph.D. thesis, Georgia Institute of Technology, Atlanta, GA.
- [85] Mayo, S. L., Olafson, B. D., and Goddard, W. A., III, 1990, "Dreiding: A Generic Force Field for Molecular Simulations," *J. Phys. Chem.*, **94**, pp. 8897–8909.
- [86] Milchev, A., Paul, W., and Binder, K., 1993, "Off-Lattice Monte Carlo Simulation of Dilute and Concentrated Polymer Solutions Under Theta Conditions," *J. Chem. Phys.*, **99**, pp. 4786–4798.
- [87] Milchev, A., Binder, K., and Bhattacharya, A., 2004, "Polymer Translocation Through a Nanopore Induced by Adsorption: Monte Carlo Simulation of a Coarse-Grained Model," *J. Chem. Phys.*, **121**, pp. 6042–6051.
- [88] Gibbons, T. G., and Klein, M. L., 1973, "Thermodynamic Properties for a Simple Model of Solid Carbon Dioxide: Monte Carlo, Cell Model, and Quasi-harmonic Calculations," *J. Chem. Phys.*, **60**, pp. 112–126.
- [89] Brooks, B. R., Bruccoleri, R. E., Olafson, B. D., States, D. J., Swaminathan, S., and Karplus, M. J., 1983, "CHARMM: A Program for Macromolecular Energy, Minimization, and Dynamics Calculations," *J. Comput. Chem.*, **4**, pp. 187–217.
- [90] Nilsson, L., and Karplus, M., 1986, "Empirical Energy Functions for Energy Minimization and Dynamics of Nucleic Acids," *J. Comput. Chem.*, **7**, pp. 591–616.
- [91] Cornell, W. D., Cieplak, P., Bayly, C. I., Gould, I. K., Merz, K. M., Jr., Ferguson, D. M., Spellmeyer, D. C., Fox, T., Caldwell, J. W., and Kollman, P. A., 1995, "A Second Generation Force Field for the Simulation of Proteins and Nucleic Acids," *J. Am. Chem. Soc.*, **117**, pp. 5179–5197.
- [92] De Gennes, P.-G., 1979, *Scaling Concepts in Polymer Physics*, Cornell University Press, London.
- [93] Theodorou, D. N., 2004, "Understanding and Predicting Structure-Property Relations in Polymeric Materials Through Molecular Simulations," *Mol. Phys.*, **102**, pp. 147–166.
- [94] Carmesin, I., and Kremer, K., 1988, "The Bond Fluctuation Method: A New Effective Algorithm for the Dynamics of Polymers in All Spatial Dimensions," *Macromolecules*, **21**, pp. 2819–2823.
- [95] Hoogerbrugge, P. J., and Koelman, J. M. V. A., 1992, "Simulating Microscopic Hydrodynamic Phenomena With Dissipative Particle Dynamics," *Europhys. Lett.*, **19**, pp. 155–160.
- [96] Baschnagel, J., Binder, K., Paul, W., Laso, M., Suter, U. W., Batoulis, I., Jilge, W., and Bürger, T., 1991, "On the Construction of Coarse-Grained Models for Linear Flexible Polymer Chains: Distribution Functions for Groups of Consecutive Monomers," *J. Chem. Phys.*, **95**, pp. 6014–6025.
- [97] Meyer, H., Biermann, O., Faller, R., Reith, D., and Müller-Plathe, F., 2000, "Coarse Graining of Nonbonded Inter-Particle Potentials Using Automatic Simplex Optimization to Fit Structural Properties," *J. Chem. Phys.*, **113**, pp. 6264–6275.
- [98] Abrams, C. F., and Kremer, K., 2003, "Combined Coarse-Grained and Atomistic Simulation of Liquid Bisphenol A-Polycarbonate: Liquid Packing and Intramolecular Structure," *Macromolecules*, **36**, pp. 260–267.
- [99] Abrams, C. F., and Kremer, K., 2001, "The Effect of Bond Length on the Structure of Dense Bead-Spring Polymer Melts," *J. Chem. Phys.*, **115**, pp. 2776–2785.
- [100] Kremer, K., and Müller-Plathe, F., 2001, "Multiscale Problems in Polymer Science: Simulation Approaches," *MRS Bull.*, **26**(3), pp. 205–210.
- [101] Fetisko, S. W., and Cummings, P. T., 2007, "Brownian Dynamics Simulation of Bead-Spring Chain Models for Dilute Polymer Solutions in Elongational Flow," *J. Rheol.*, **32**, pp. 285–298.
- [102] Koelman, J. M. V. A., and Hoogerbrugge, P. J., 1993, "Dynamic Simulations of Hard-Sphere Suspensions Under Steady Shear," *Europhys. Lett.*, **21**(3), pp. 363–368.
- [103] Groot, R. D., and Warren, P. B., 1997, "Dissipative Particle Dynamics: Bridging the Gap Between Atomistic and Mesoscopic Simulation," *J. Chem. Phys.*, **107**(11), pp. 4423–4435.
- [104] Español, P., 1998, "Fluid Particle Model," *Phys. Rev. E*, **57**(3), pp. 2930–2948.
- [105] Altevogt, P., Evers, O. A., Fraaij, J. G. E. M., Maurits, N. M., and van Vliemmeren, B. A. C., 1999, "The MesoDyn Project: Software for Mesoscale Chemical Engineering," *J. Mol. Struct.: THEOCHEM*, **463**, pp. 139–143.
- [106] Hännigi, P., Talkner, P., and Borkovec, M., 1990, "Reaction-Rate Theory: Fifty Years After Kramers," *Rev. Mod. Phys.*, **62**(2), pp. 251–341.
- [107] Voter, A. F., 1997, "A Method for Accelerating the Molecular Dynamics Simulation of Infrequent Events," *J. Chem. Phys.*, **106**(11), pp. 4665–4677.
- [108] Voter, A. F., 1997, "Hyperdynamics: Accelerated Molecular Dynamics of Infrequent Events," *Phys. Rev. Lett.*, **78**(20), pp. 3908–3911.
- [109] Henkelman, G., and Jónsson, H., 2001, "Long Time Scale Kinetic Monte Carlo Simulations Without Lattice Approximation and Predefined Event Table," *J. Chem. Phys.*, **115**(21), pp. 9657–9666.
- [110] Sørensen, M. R., and Voter, A. F., 2000, "Temperature-Accelerated Dynamics for Simulation of Infrequent Events," *J. Chem. Phys.*, **112**(21), pp. 9599–9606.
- [111] Grimmelmann, E. K., Tully, J. C., and Helfand, E., 1981, "Molecular Dynamics of Infrequent Events: Thermal Desorption of Xenon From a Platinum Surface," *J. Chem. Phys.*, **74**(9), pp. 5300–5310.
- [112] Steiner, M. M., Genilloud, P.-A., and Wilkins, J. W., 1998, "Simple Bias Potential for Boosting Molecular Dynamics With the Hyperdynamics Scheme," *Phys. Rev. B*, **57**(17), pp. 10236–10239.
- [113] Gong, X. G., and Wilkins, J. W., 1999, "Hyper Molecular Dynamics With a Local Bias Potential," *Phys. Rev. B*, **59**(1), pp. 54–57.
- [114] Duan, X. M., and Gong, X. G., 2003, "Local Bias Potential in Hyper Molecular Dynamics Method," *Comput. Mater. Sci.*, **27**, pp. 375–380.
- [115] Hutnik, M., Gentile, F. T., Ludovice, P. J., Suter, U. W., and Argon, A. S., 1991, "An Atomistic Model of the Amorphous Glassy Polycarbonate of 4,4-Isopropylidenediphenol," *Macromolecules*, **24**, pp. 5962–5969.
- [116] Verdier, P. H., 1966, "Monte Carlo Studies of Lattice-Model Polymer Chains. II. End-to-End Length," *J. Chem. Phys.*, **45**, pp. 2122–2128.
- [117] Hilhorst, H. J., and Deutch, J. M., 1975, "Analysis of Monte Carlo Results on the Kinetics of Lattice Polymer Chains With Excluded Volume," *J. Chem. Phys.*, **63**, pp. 5153–5161.
- [118] Baschnagel, J., Binder, K., and Wittmann, H.-P., 1993, "The Influence of the Cooling Rate on the Glass Transition and the Glassy State in Three-Dimensional Dense Polymer Melts: A Monte Carlo Study," *J. Phys.: Condens. Matter*, **5**, pp. 1597–1618.
- [119] Tries, V., Paul, W., Baschnagel, J., and Binder, K., 1996, "Modeling Polyethylene With the Bond Fluctuation Model," *J. Chem. Phys.*, **106**, pp. 738–748.
- [120] Kremer, K., Grest, G. S., and Carmesin, I., 1988, "Crossover From Rouse to Reptation Dynamics: A Molecular-Dynamics Simulation," *Phys. Rev. Lett.*, **61**, pp. 566–569.
- [121] Jäckle, J., 1986, "Models of the Glass Transition," *Rep. Prog. Phys.*, **49**, pp. 171–231.
- [122] Kremer, K., and Grest, G. S., 1990, "Dynamics of Entangled Linear Polymer Melts: A Molecular-Dynamics Simulation," *J. Chem. Phys.*, **92**, pp. 5057–5086.
- [123] de Gennes, P. G., 1979, *Scaling Concepts in Polymer Physics*, Cornell University Press, Ithaca, NY.
- [124] Doi, M., and Edwards, S. F., 1986, *The Theory of Polymer Dynamic*, Clarendon, Oxford.
- [125] Kavassalis, T. A., and Sundararajan, P. R., 1993, "A Molecular Dynamics Study of Polyethylene Crystallization," *Macromolecules*, **26**, pp. 4144–4150.
- [126] Bergström, J. S., and Boyce, M. C., 2001, "Deformation of Elastomeric Networks: Relation Between Molecular Level Deformation and Classical Statistical Mechanics Models of Rubber Elasticity," *Macromolecules*, **32**, pp. 3795–3808.
- [127] Capaldi, F. M., Boyce, M. C., and Rutledge, G. C., 2002, "Enhanced Mobility Accompanies the Active Deformation of a Glassy Amorphous Polymer," *Phys. Rev. Lett.*, **89**, p. 175505.
- [128] Yashiro, K., Ito, T., and Tomita, Y., 2003, "Molecular Dynamics Simulation of Deformation Behavior in Amorphous Polymer: Nucleation of Chain Entanglements and Network Structure Under Uniaxial Tension," *Int. J. Mech. Sci.*, **45**, pp. 1863–1876.

- [129] Valavala, P. K., Clancy, T. C., Odegard, G. M., and Gates, T. S., 2007, "Nonlinear Multiscale Modeling of Polymer Materials," *Int. J. Solids Struct.*, **44**, pp. 1161–1179.
- [130] Valavala, P. K., Clancy, T. C., Odegard, G. M., Gates, T. S., and Aifantis, E. C., 2009, "Multiscale Modeling of Polymer Materials Using a Statistics-Based Micromechanics Approach," *Acta Mater.*, **57**, pp. 525–532.
- [131] Shenogin, S., and Ozisik, R., 2005, "Simulation of Plastic Deformation in Glassy Polymers: Atomistic and Mesoscale Approaches," *J. Polym. Sci., Part B: Polym. Phys.*, **43**, pp. 994–1004.
- [132] Kroner, E., 1960, "Allgemeine kontinuumstheorie der versetzungen und eigenspannungen," *Arch. Ration. Mech. Anal.*, **4**, pp. 273–334.
- [133] Lee, E. H., 1969, "Elastic Plastic Deformation at Finite Strain," *ASME J. Appl. Mech.*, **36**, pp. 1–6.
- [134] Anand, L., and Gurtin, M. E., 2003, "A Theory of Amorphous Solids Undergoing Large Deformations, With Application to Polymeric Glasses," *Int. J. Solids Struct.*, **40**, pp. 1465–1487.
- [135] Boyce, M. C., Weber, G. G., and Parks, D. M., 1989, "On the Kinematics of Finite Strain Plasticity," *J. Mech. Phys. Solids*, **37**(5), pp. 647–665.
- [136] Gurtin, M. E., and Anand, L., 2005, "The Decomposition  $F = F_e F_p$ , Material Symmetry, and Plastic Irrotationality for Solids that Are Isotropic-Viscoplastic or Amorphous," *Int. J. Plast.*, **21**, pp. 1686–1719.
- [137] Holzapfel, G. A., 2000, *Nonlinear Solid Mechanics. A Continuum Approach for Engineering*, Wiley, New York.
- [138] Callen, H. B., 1985, *Thermodynamics and an Introduction to Thermostatistics*, 2nd ed., Wiley, New York.
- [139] Coleman, B., and Gurtin, M., 1967, "Thermodynamics With Internal State Variables," *J. Chem. Phys.*, **47**, pp. 597–613.
- [140] Germain, P., Nguyen, Q. S., and Suquet, P., 1983, "Continuum Thermodynamics," *Trans. ASME, J. Appl. Mech.*, **50**, pp. 1010–1020.
- [141] Lemaitre, J., and Chaboche, J. L., 1990, *Mechanics of Solid Materials*, Cambridge University Press, England.
- [142] Lubliner, J., 1990, *Plasticity Theory*, Macmillan, New York.
- [143] Maugin, G. A., 1992, *The Thermomechanics of Plasticity and Fracture*, Cambridge University Press, Cambridge, England.
- [144] Bathe, K., 1982, *Finite Element Procedure in Engineering Analysis*, Prentice-Hall, Englewood Cliffs, NJ.
- [145] Zienkiewicz, O., 1977, *The Finite Element Method*, McGraw-Hill, New York.
- [146] Belytschko, T., Liu, W. K., and Moran, B., 2000, *Nonlinear Finite Element for Continua and Structures*, Wiley, New York.
- [147] Van der Sluis, O., Schreurs, P. J. G., and Meijer, H. E. H., 2001, "Homogenisation of Structured Elastoviscoplastic Solids at Finite Strains," *Mech. Mater.*, **33**, pp. 499–522.
- [148] Perzyna, P., 1966, "Fundamental Problems in Viscoplasticity," *Adv. Appl. Mech.*, **9**, pp. 243–377.
- [149] Krempl, E., 1995, "The Overstress Dependence of the Inelastic Rate of Deformation Inferred From Transient Tests," *Mater. Sci. Res. Int.*, **1**, pp. 3–10.
- [150] Krempl, E., 1996, "A Small Strain Viscoplasticity Theory Based on Overstress," *Unified Constitutive Laws of Plastic Deformation*, A. Krausz and K. Krausz, eds., Academic Press, San Diego, pp. 281–318.
- [151] Krempl, E., and Ho, K., 2000, "An Overstress Model for Solid Polymer Deformation Behavior Applied to Nylon 66," *Time Dependent and Nonlinear Effects in Polymers and Composites*, ASTM STP, 1357, pp. 118–137.
- [152] Krempl, E., and Khan, F., 2003, "Rate (Time)-Dependent Deformation Behavior: An Overview of Some Properties of Metals and Solid Polymers," *Int. J. Plast.*, **19**, pp. 1069–1095.
- [153] Colak, O. U., 2005, "Modeling Deformation Behavior of Polymers With Viscoplasticity Theory Based on Overstress," *Int. J. Plast.*, **21**, pp. 145–160.
- [154] Christensen, R. M., 1982, *Theory of Viscoelasticity: An Introduction*, Academic, New York.
- [155] Lubarda, V. A., Benson, D. J., and Meyers, M. A., 2003, "Strain-Rate Effects in Rheological Models of Inelastic Response," *Int. J. Plast.*, **19**, pp. 1097–1118.
- [156] Bardenhagen, S. G., Stout, M. G., and Gray, G. T., 1997, "Three-Dimensional Finite Deformation Viscoplastic Constitutive Models for Polymeric Materials," *Mech. Mater.*, **25**, pp. 235–253.
- [157] Khan, A. S., and Zhang, H., 2001, "Finite Deformation of a Polymer and Constitutive Modeling," *Int. J. Plast.*, **17**, pp. 1167–1188.
- [158] Khan, A. S., Lopez-Pamies, O., and Kazmi, R., 2006, "Thermo-Mechanical Large Deformation Response and Constitutive Modeling of Viscoelastic Polymers Over a Wide Range of Strain Rates and Temperatures," *Int. J. Plast.*, **22**, pp. 581–601.
- [159] Leonov, A. I., 1976, "Nonequilibrium Thermodynamics and Rheology of Viscoelastic Polymer Media," *Rheol. Acta*, **15**, pp. 85–98.
- [160] Tervoort, T. A., Smit, R. J. M., Brekelmans, W. A. M., and Govaert, L. E., 1998, "A Constitutive Equation for the Elasto-Viscoplastic Deformation of Glassy Polymers," *Mech. Time-Depend. Mater.*, **1**, pp. 269–291.
- [161] Tervoort, T. A., and Govaert, L. E., 2000, "Strain-Hardening Behavior of Polycarbonate in the Glassy State," *J. Rheol.*, **44**, pp. 1263–1277.
- [162] Govaert, L. E., Timmermans, P. H. M., and Brekelmans, W. A. M., 2000, "The Influence of Intrinsic Strain Softening on Strain Localization in Polycarbonate: Modeling and Experimental Validation," *ASME J. Eng. Mater. Technol.*, **122**, pp. 177–185.
- [163] Chaboche, J. L., 1997, "Thermodynamic Formulation of Constitutive Equations and Application to the Viscoplasticity and Viscoelasticity of Metals and Previous Termpolymers," *Int. J. Solids Struct.*, **34**, pp. 2239–2254.
- [164] Frank, G. J., and Brockman, R. A., 2001, "A Viscoelastic-Viscoplastic Constitutive Model For Glassy Polymers," *Int. J. Solids Struct.*, **38**, pp. 5149–5164.
- [165] Zairi, F., Naït-Abdelaziz, M., Woznica, K., and Gloaguen, J. M., 2007, "Elasto-Viscoplastic Constitutive Equations for the Description of Glassy Polymer Behavior at Constant Strain Rate," *ASME J. Eng. Mater. Technol.*, **129**(1), pp. 29–35.
- [166] Anand, L., and Ames, N. M., 2006, "On Modeling the Micro-Indentation Response of an Amorphous Polymer," *Int. J. Plast.*, **22**, pp. 1123–1170.
- [167] Haward, R. N., and Thackray, G., 1968, "The Use of a Mathematical Model to Describe Isothermal Stress-Strain Curves in Glassy Thermoplastics," *Proc. R. Soc. London, Ser. A*, **302**, pp. 453–472.
- [168] Eyring, H., 1936, "Viscosity, Plasticity, and Diffusion as Examples of Absolute Reaction Rates," *J. Chem. Phys.*, **4**, pp. 283–291.
- [169] James, H. M., and Guth, E., 1943, "Theory of Elastic Properties of Rubber," *J. Chem. Phys.*, **11**, pp. 455–481.
- [170] Boyce, M. C., Parks, D. M., and Argon, A. S., 1988, "Large Inelastic Deformation of Glassy Deformation of Glassy Polymers Part I: Rate Dependent Constitutive Model," *Mech. Mater.*, **7**, pp. 15–33.
- [171] Argon, A. S., 1973, "A Theory for the Low Temperature Plastic Deformation of Glassy Polymers," *Philos. Mag.*, **28**, pp. 839–865.
- [172] Robertson, R. E., 1966, "Theory for the Plasticity of Glassy Polymers," *J. Chem. Phys.*, **44**, pp. 3950–3956.
- [173] Ree, T., and Eyring, H., 1955, "Theory of Non-Newtonian Flow. I. Solid Plastic System," *J. Appl. Phys.*, **26**, pp. 793–800.
- [174] Ree, T., and Eyring, H., 1958, *Rheology*, Vol. III, Academic, New York.
- [175] Fotheringham, D. G., and Cherry, B. W., 1976, "Comment on the Compression Yield Behaviour of Polymethyl Methacrylate Over a Wide Range of Temperatures and Strain-Rates," *J. Mater. Sci.*, **11**, pp. 1368–1370.
- [176] Fotheringham, D. G., and Cherry, B. W., 1978, "The Role of Recovery Forces in the Deformation of Linear Polyethylene," *J. Mater. Sci.*, **13**, pp. 951–964.
- [177] Ogden, R. W., 1972, "Large Deformation Isotropic Elasticity—On the Correlation of Theory and Experiment for Incompressible Rubberlike Solids," *Proc. R. Soc. London, Ser. A*, **326**, pp. 565–584.
- [178] Rivlin, R. S., and Saunders, D. W., 1951, "Large Elastic Deformations of Isotropic Materials VII. Experiments on the Deformation of Rubber," *Philos. Trans. R. Soc. London, Ser. A*, **243**(865), pp. 251–2881.
- [179] Yeoh, O. H., 1990, "Characterization of Elastic Properties of Carbon-Black-Filled Rubber Vulcanizates," *Rubber Chem. Technol.*, **63**, pp. 792–805.
- [180] Gent, A. N., 1996, "A New Constitutive Relation for Rubber," *Rubber Chem. Technol.*, **69**, pp. 59–61.
- [181] Arruda, E. M., and Boyce, M. C., 1993, "A Three-Dimensional Constitutive Model for the Large Stretch Behavior of Rubber Elastic Materials," *J. Mech. Phys. Solids*, **41**, pp. 389–412.
- [182] Wu, P. D., and Van der Giessen, E., 1993, "On Improved Network Models for Rubber Elasticity and Their Applications to Orientation Hardening in Glassy Polymers," *J. Mech. Phys. Solids*, **41**, pp. 427–456.
- [183] Elias-Zuniga, A., and Beatty, M. F., 2002, "Constitutive Equations for Amended Non-Gaussian Network Models of Rubber Elasticity," *Int. J. Eng. Sci.*, **40**, pp. 2265–2294.
- [184] Miehe, C., Goktepe, S., and Mendez Diez, J., 2008, "Finite Viscoplasticity of Amorphous Glassy Polymers in the Logarithmic Strain Space," *Int. J. Solids Struct.*, **46**, pp. 181–202.
- [185] Mulliken, A. D., and Boyce, M. C., 2006, "Mechanics of the Rate-Dependent Elastic-Plastic Deformation of Glassy Polymers From Low to High Strain Rates," *Int. J. Solids Struct.*, **43**, pp. 1331–1356.
- [186] Richeton, J., Ahzi, S., Vecchio, K. S., Jiang, F. C., and Makradi, A., 2007, "Modeling and Validation of the Large Deformation Inelastic Response of Amorphous Polymers Over a Wide Range of Temperatures and Strain Rates," *Int. J. Solids Struct.*, **44**, pp. 7938–7954.
- [187] Hasan, O. A., Boyce, M. C., Li, X. S., and Berko, S., 1993, "An Investigation of the Yield and Postyield Behavior and Corresponding Structure of Poly(Methyl Methacrylate)," *J. Polym. Sci., Part B: Polym. Phys.*, **31**, pp. 185–197.
- [188] Hasan, O. A., and Boyce, M. C., 1995, "A Constitutive Model for the Non-linear Viscoelastic Viscoplastic Behavior of Glassy Polymers," *Polym. Eng. Sci.*, **35**, pp. 331–344.
- [189] McDowell, D., 2005, "Internal State Variable Theory," *Handbook of Materials Modeling, Part A: Methods*, S. Yip and M. F. Horstemeyer, eds., Springer, The Netherlands, pp. 1151–1170.
- [190] Follansbee, P., and Cocks, U., 1988, "A Constitutive Description of the Deformation of Copper Based on the Use of the Mechanical Threshold Stress as an Internal State Variable," *Acta Metall.*, **36**, pp. 81–93.
- [191] Horstemeyer, M., 1998, "Damage Influence on Bauschinger Effect of a Cast A356 Aluminum Alloy," *Scr. Mater.*, **39**, pp. 1491–1495.
- [192] Horstemeyer, M., 2001, "From Atoms to Autos: Part 2: Monotonic Loads," Sandia National Laboratories, Report No. SAND2001-8662.
- [193] McDowell, D., 1985, "Two Surface Model for Transient Nonproportional Cyclic Plasticity: Part 1. Development of Appropriate Equations," *ASME J. Appl. Mech.*, **52**, pp. 298–302.
- [194] Horstemeyer, M., 2002, "High Cycle Fatigue Mechanisms in a Cast AM60B Magnesium Alloy," *Fatigue Fract. Eng. Mater. Struct.*, **25**, pp. 1045–1056.
- [195] Gall, K., and Horstemeyer, M., 2000, "Integration of Basic Materials Research Into the Design of Cast Components by a Multiscale Methodology," *ASME J. Eng. Mater. Technol.*, **122**, pp. 355–362.
- [196] Horstemeyer, M. F., Lathrop, J., Gokhale, A. M., and Dighe, M., 2000, "Modeling Stress State Dependent Damage Evolution in a Cast Al-Si-Mg Aluminum Alloy," *Theor. Appl. Fract. Mech.*, **33**, pp. 31–47.
- [197] Horstemeyer, M., Plimpton, S., and Baskes, M., 2001, "Length Scale and



- Time Scale Effects on the Plastic Flow of fcc Metals,” *Acta Mater.*, **49**, pp. 4363–4374.
- [198] Schapery, R. A., 1999, “Nonlinear Viscoelastic and Viscoplastic Constitutive Equations With Growing Damage,” *Int. J. Fract.*, **97**, pp. 33–66.
- [199] Yoon, C., and Allen, D. H., 1999, “Damage Dependent Constitutive Behavior and Energy Release Rate for a Cohesive Zone in a Thermoviscoelastic Solid,” *Int. J. Fract.*, **96**, pp. 55–74.
- [200] Wei, P. J., and Chen, J. K., 2003, “A Viscoelastic Constitutive Model With Nonlinear Evolutionary Internal Variables,” *Acta Mech.*, **164**, pp. 217–225.
- [201] Ghorbel, E., 2008, “A Viscoplastic Constitutive Model for Polymeric Materials,” *Int. J. Plast.*, **24**, pp. 2032–2058.
- [202] Anand, L., Ames, N. M., Srivastava, V., and Chester, S. C., 2009, “A Thermo-Mechanically Coupled Theory for Large Deformations of Amorphous Polymers. Part I: Formulation,” *Int. J. Plast.*, **25**, pp. 1474–1494.
- [203] Ames, N. M., Srivastava, V., Chester, S. C., and Anand, L., 2009, “A Thermo-Mechanically Coupled Theory for Large Deformations of Amorphous Polymers. Part II: Applications,” *Int. J. Plast.*, **25**, pp. 1495–1539.
- [204] Theodorou, D. N., 2004, “Understanding and Predicting Structure-Property Relations in Polymeric Materials Through Molecular Simulations,” *Molecular Physics Foundations of Molecular Modeling and Simulation FOMMS 2003*, Taylor & Francis, London, Vol. 102(2, part 1), pp. 147–166.
- [205] Theodorou, D. N., 2007, “Hierarchical Modelling of Polymeric Materials,” *Chem. Eng. Sci.*, **62**, pp. 5697–5714.